Original Paper

Pharmacology

Pharmacology 2009;84:42–60
DOI: 10.1159/000227286

Received: December 16, 2008
Accepted: April 27, 2009
Published online: July 4, 2009

SD0006: A Potent, Selective and Orally Available Inhibitor of p38 Kinase

Barry L. Burnette Shaun Selness Raj Devraj Gail Jungbluth Ravi Kurumbail Loreen Stillwell Gary Anderson Stephen Mnich Jeffrey Hirsch Robert Compton Pamela De Ciechi Heidi Hope Michael Hepperle Robert H. Keith Win Naing Huey Shieh Joseph Portanova Yan Zhang Jian Zhang Richard M. Leimgruber Joseph Monahan

Pfizer Global Research and Development, Pfizer, Chesterfield, Mo., USA

Key Words
p38 kinase · Rheumatoid arthritis · Arthritis · Inflammation · Diarylpyrazole · SD0006

Abstract
SD0006 is a diarylpyrazole that was prepared as an inhibitor of p38 kinase-α (p38α). In vitro, SD0006 was selective for p38α kinase over 50 other kinases screened (including p38γ and p38δ with modest selectivity over p38β). Crystal structures with p38α show binding at the ATP site with additional residue interactions outside the ATP pocket unique to p38α that can confer advantages over other ATP competitive inhibitors. Direct correlation between inhibition of p38α activity and that of lipopolysaccharide-stimulated TNFα release was established in cellular models and in vivo, including a phase 1 clinical trial. Potency (IC_{50}) for inhibiting tumor necrosis factor-α (TNFα) release, in vitro and in vivo, was <200 nmol/l. In vivo, SD0006 was effective in the rat streptococcal-cell-wall-induced arthritis model, with dramatic protective effects on paw joint integrity and bone density as shown by radiographic analysis. In the murine collagen-induced arthritis model, equivalence was demonstrated to anti-TNFα treatment. SD0006 also demonstrated good oral anti-inflammatory efficacy with excellent cross-species correlation between the rat, cynomolgus monkey, and human. SD0006 suppressed expression of multiple proinflammatory proteins at both the transcriptional and translational levels. These properties suggest SD0006 could provide broader therapeutic efficacy than cytokine-targeted monotherapeutics.

Introduction

The pathology of many diseases such as rheumatoid arthritis (RA), Crohn's disease, chronic obstructive pulmonary disease and diabetes is the result of chronic inflammation mediated by proinflammatory cytokines [1–3]. Biological agents (such as Enbrel, Remicade, Humira and Kineret) that sequester tumor necrosis factor-α (TNFα) or interleukin-1β (IL-1β) have proven very useful therapeutics for RA and are being evaluated for other inflammation-mediated diseases [1, 4–9]. However, these agents are expensive, parenterally administered, and ineffective in a substantial minority of those who try them [10, 11]. They are also under review for increased risk of cancer, infection, multiple sclerosis, and for the potential to induce neutralizing antibodies over the long term [12–15].

The α-isoform of mitogen-activated protein kinase (MAPK) p38 (p38α) is the most abundant isoform in in-

KARGER

Fax +41 61 306 12 34
E-Mail karger@karger.ch
www.karger.com

0031–7012/09/0841–0042$26.00/0

Accessible online at:
www.karger.com/pha

Barry L. Burnette, PhD
Pfizer Global Research and Development, Pfizer, Inc.
700 Chesterfield Parkway North, BB4A
Chesterfield, MO 63017 (USA)
Tel. +1 636 247 6907, Fax +1 636 247 6511, E-Mail barry.l.burnette@pfizer.com

flammatory cells [16] and is involved in both the transcriptional and translational control of proinflammatory proteins involved in the inflammatory response, including TNFα, IL-1β, and IL-6 [17–21]. The subsequent responses that TNFα and IL-1β transmit through their respective receptors lead to induction of additional proinflammatory proteins involved in the pathogenesis of RA that are also mediated through p38α, including induction of cyclooxygenase 2 (COX-2), matrix metalloproteases (MMPs) 1, 3 and 9, receptor activator of nuclear factor NF-κB ligand (RANKL), inducible nitric oxide synthase (iNOS), and integrin expression [20, 22–30]. Selective inhibitors of p38α block the production and activity of these proteins and have demonstrated marked efficacy in animal models of acute inflammation, arthritis and chronic obstructive pulmonary disease [2, 25, 31–36]. The ability of p38α inhibitors to reduce the levels of multiple inflammatory cytokines and mediator proteins suggests that these compounds have the potential for enhanced and/or broader efficacy compared with agents restricted to single-cytokine modulation.

Interest in p38α as a target for therapeutic drug intervention has been high in the pharmaceutical industry [37, 38]. Early p38α inhibitor patents focused on imidazole-based compounds [39, 40] and were followed by patents claiming structures based on pyrroles, thiazoles, and oxazoles [35, 41], and others with unrelated structures such as the pyrazole ureas [34, 36, 42, 43]. We report here on the preclinical biological evaluation and phase 1 clinical evaluation of SD0006, a diarylpyrazole (DAP). SD0006 is highly selective for p38α, suppresses expression of multiple proinflammatory proteins, and ameliorates disease severity in animal models of arthritis with good oral bioavailability. Using lipopolysaccharide (LPS)-induced activation, a direct correlation was demonstrated between inhibition of p38α activity and TNFα release, both ex vivo with monocytic cells and human whole blood (HWB), and in vivo via experimental endotoxemia in rodents and humans.

Materials and Methods

Synthesis of DAPs

Synthesis will be published later.

Reagents

Following are the antibodies used, listed by the antigen they were targeted against with the supplier in parentheses: heat shock protein 27(Hsp27), extracellular regulated kinase (ERK), p38α, and cJun N-terminal kinase (JNK; Santa Cruz Biotechnology, Santa Cruz, Calif., USA); MAPK activated protein kinase 2(MK-2), Thr 334 and Thr 222 of MK-2, and phospho-ERK (Cell Signaling Technology, Beverly, Mass., USA); phospho-p38α and phospho-JNK (Biosource International, Camarillo, Calif., USA); phospho-Hsp27 (Upstate Biotechnology, Lake Placid, N.Y., USA); p38 β-, δ-, and γ-isoform specific (Quality Controlled Biochemicals, Hopkinton, Mass., USA); COX-1 (Cayman Laboratories, Ann Arbor, Mich., USA); COX-2 (Oxford Biomedical Research, Oxford, Mich., USA). SC74102, 4-(3-(4-fluorophenyl)-1H-pyrazol-4-yl)-pyridine; SC79659, 1-(4-(3-(4-chlorophenyl)-4-(pyridin-4-yl)-1H-pyrazol-5-yl)piperidin-1-yl)-2-hydroxyethanone; SD0006, 1-(4-(3-(4-chlorophenyl)-4-(pyrimidin-4-yl)-1H-pyrazol-5-yl)-piperidin-1-yl)-2-hydroxyethanone; and SC79409, 4-(3-(4-chlorophenyl)-5-(1-methylpiperidin-4-yl)-1H-pyrazol-4-yl)pyrimidine, were DAP compounds synthesized by Pfizer (St. Louis, Mo., USA) and stored as powders. Biotinylated Hsp27 peptide substrate was provided by American Peptide Company (Sunnyvale, Calif., USA). All other chemicals were obtained commercially and were of the highest purity available.

Cytokine and Prostaglandin E_2 Assays

Plasma from clinical trials was assayed for TNFα and IL-6 with Linco (St. Charles, Mo., USA) human cytokine detection kits as per the manufacturer's instructions. Cytokines were quantitated using the Luminex100 (Luminex Corporation, Toronto, Ont., Canada). TNFα concentrations were extrapolated from recombinant protein standard curves using a BioAssay Solver Macro (statistical software program developed internally at Pfizer) with a four-parameter logistic model.

For U937 cell and human peripheral blood primary monocyte assays, and plasma from the HWB ex vivo assay, the Meso Scale Discovery (Gaithersburg, Md., USA) electrochemiluminescence human proinflammatory 4-plex (TNFα, IL-6, IL-1β, and IL-8) kit was used. Plasma levels of monkey TNFα were quantitated by a human TNFα enzyme-linked immunosorbent assay (ELISA) kit (Pharmingen, San Diego, Calif., USA) that detects human TNFα with a sensitivity of 7.5 pg/ml. For TNFα from rat plasma an in-house protocol was developed. Briefly, ELISA plates were coated with hamster antimouse/rat TNFα monoclonal antibody TN19.12 provided by Dr. Robert Schreiber (Washington University, St. Louis, Mo., USA), then blocked with gelatin in phosphate-buffered saline (PBS). Diluted serum samples were added to wells, incubated and washed; then rabbit antimouse/rat TNFα antibody (BioSource) was added. After incubation and washing, peroxidase-conjugated donkey antirabbit IgG antibody (Jackson ImmunoResearch, West Grove, Pa., USA) was added, incubated and washed again, and then developed with 2,2′-azino-di(3-ethylbenzthiazoline-6-sulfonate)-peroxide solution (Kirkegaard and Perry Laboratories, Gaithersburg, Md., USA) before reading in a SpectroMax 340 spectrophotometer (Molecular Devices Corp., Sunnyvale, Calif., USA) at 405 nm. TNFα levels in rat serum were quantitated from a recombinant rat TNFα (BioSource International) standard curve using a quadratic parameter fit generated by SoftMaxPRO 5 software (Molecular Devices). Sensitivity was approximately 30 pg TNFα/ml. PGE_2 assays used ELISA kits from Cayman as per the manufacturer's instructions. Half-maximal inhibitory concentration (IC_{50}) and median effective dose (ED_{50}) values were generated using Grafit 5(2) software (Erithacus Software, Horley, UK).

Cell-Based Assays

U937 Cells and Human Peripheral Blood Mononuclear Cells

The U937 human premonocytic cell line was obtained from the American Type Culture Collection (Rockville, Md., USA). U937 cells were grown in RPMI-1640 with glutamine, penicillin-streptomycin (10 U/ml) and 10% heat-inactivated fetal bovine serum (FBS). Cells were differentiated to a monocyte/macrophage phenotype with phorbol myristate acetate (Sigma Chemical, St. Louis, Mo., USA; 20 ng/ml, 24 h), washed and rested 48 h prior to stimulation with LPS (*Escherichia coli* serotype 011:B4) as described below.

Primary human monocytes were obtained from venous blood of donors collected anonymously at an on-site clinic into sodium heparin tubes and used immediately. Peripheral blood mononuclear cells were prepared by density gradient centrifugation using Histopaque 1077 (Sigma) as per the manufacturer's directions. Monocytes were then prepared by negative magnetic bead selection using the Monocyte Isolation Kit II with the autoMACS separator as per the manufacturer's specifications (both by Miltenyi Biotec, Bergisch Gladbach, Germany).

LPS Stimulation of U937 Cells and Human Primary Monocytes

DAP was added to phorbol-myristate-acetate-differentiated U937 cells 1 h prior to LPS stimulation. For signaling studies, cells were stimulated with LPS (1 ng/ml) for a period of 30 min (a time previously determined to be optimal) followed by rapid lysis and nuclear digestion (as described under 'Preparing Lysates' below). Lysates were stored frozen for later assay of p38α activation. For TNFα assays, cells were stimulated with LPS (1 ng/ml) for 4 h (a time previously determined to be optimal) and cell supernatants were collected for determination of TNFα levels by ELISA. For IL-1β, stimulation was for 16 h for monocytes and U937 cells. For IL-6, stimulation was for 4 h for monocytes and 16 h for U937 cells.

RA Synovial Fibroblast Cell Line

RA synovial fibroblast (RASF) cells were derived from the inflamed synovium of a female RA patient who was undergoing total knee replacement. Cells were cultured in Dulbecco's modified Eagle's medium with 15% FBS, 1% glutamine, and 1% penicillin/streptomycin [all from Gibco (Invitrogen), Gaithersburg, Md., USA]. Experiments were performed with cells between passages 7 and 10, using trypsin with 0.25% ethylene diamine tetraacetic acid (Gibco) to detach cells.

IL-1β Stimulation of RASFs

RASFs were incubated with or without SD0006 for 1 h before 1 ng/ml IL-1β stimulation at 37°C for 20 h for induction of PGE_2, 0.5 h for phosphorylation studies, and 4 h for COX-2 expression. PGE_2 levels in culture supernatants were quantitated by ELISA, and protein expression (COX-1 and -2) and phosphorylation (of p38α, ERK, JNK, and cJun) by immunoblot analyses and ELISA.

LPS-Challenged HWB Assay

Venous blood from human donors was collected in sodium heparin tubes, then 180 μl was aliquotted per well of 96-well U-bottom plates. SD0006 in dimethylsulfoxide and ethanol in PBS or vehicle was added to blood in 10-μl aliquots in serial dilutions (final dimethylsulfoxide and ethanol concentrations were 0.1 and 1.5%, respectively). After 1 h at 37°C, 10 μl of LPS in PBS was added to give a final concentration of 1 ng/ml. After 4 h of incubation at 37°C, the blood was centrifuged for 10 min at 1,800 *g* and the plasma was harvested and assayed for human TNFα or IL-6 by ELISA.

Cell Viability

RASF viability was evaluated using the 3-(4,5-dimethylthiazol-2-yl)-) diphenyl tetrazolium bromide assay (Sigma) as per the manufacturer's instructions. Absorbance was measured on an ELISA plate reader with a test wavelength of 570 nm and a reference of 630 nm.

In vivo Assays

All animal studies were approved by the St. Louis Pfizer Institutional Animal Care and Use Committee. The clinical trial was performed in accordance with the International Conference on Harmonization Good Clinical Practice guidelines, and applicable local regulatory requirements and laws.

Carrageenan-Induced Paw Inflammation

Male Sprague-Dawley rats (Charles River, Portage, Mich., USA), 170–210 g, were fasted with free access to water at least 16 h prior to testing. SD0006 (or dexamethasone as a comparator) was dosed orally in 1 ml of 0.5% methylcellulose, 0.025% Tween-20 2 h before carrageenan injection into the paw (prophylactic protocol), or dosed orally 3 h after carrageenan challenge (therapeutic protocol). Carrageenan was prepared as a 1% suspension in saline then 0.1 ml was injected into the foot pad tissue of the right hind paw while the noninjected contralateral foot pad of each animal served as a normal control in the measurement of edema and hyperalgesia. Edema was expressed as the difference (Δ) in the volume of a paw measured before carrageenan and at the termination of the experiment (determined with a plethysmometer). Hyperalgesia was quantitated by measurement of the withdrawal response (Δ withdrawal latency) to a thermal stimulus wherein the rats, individually confined to Plexiglas chambers, were exposed to light from a high-intensity projector bulb positioned beneath each hind paw. The difference in the withdrawal latency in seconds between carrageenan-injected and contralateral control paws served as a measure of pain. Paw volume and withdrawal latency were measured 3 h after carrageenan challenge in the prophylactic protocol and withdrawal latency at 1, 2 and 3 h in the therapeutic protocol. Percent inhibition = [1 – (mean treatment/mean vehicle)] × 100.

Induction and Assessment of Collagen-Induced Arthritis in Mice

8- to 12-week-old DBA/1 (Jackson Laboratory, Bar Harbor, Me., USA) mice were dosed at 3.75, 7.5, or 15 mg SD0006/kg, twice daily (b.i.d.), with aqueous methylcellulose/Tween vehicle used for comparison. Hamster antimouse monoclonal TNFα antibody (a gift from Dr. Robert Schreiber) was administered at a dose of 250 μg/week by intraperitoneal injection in saline. Arthritis was induced by injection of 50 μg of chick type II collagen (provided by Dr. Marie Griffiths, University of Utah, Salt Lake City, Utah, USA) in complete Freund's adjuvant (Sigma) on day 0 at the base of the tail. Animals were boosted on day 21 as above. Animals were evaluated several times each week for up to 8 weeks,

and any animal with paw redness or swelling was counted as arthritic. Severity was evaluated using a score of 1–3 for each paw, with any redness or swelling of digits or the paw being scored as 1, gross swelling of the whole paw or deformity as 2, and ankylosis of joints as 3 (maximal score of 12/mouse). Statistical analysis comparing the percentage of arthritis between groups was done using Fisher's exact test.

Stimulation of Cytokine Expression by Streptococcal Cell Wall

Female Lewis rats (100–140 g) received a single intraperitoneal injection of streptococcal cell wall (SCW) suspension (Lee Laboratories, Grayson, Ga., USA) at a dose of 15–60 μg rhamnose equivalents/g body weight. Treatment of rats daily with SD0006 administered orally b.i.d or with 10 mg/kg recombinant soluble rat TNFRII fused to the Fc fragment of rat IgG [sTNFRII-Fc chimera; J. O. Polazzi and J. Portanova, unpubl. obs.], administered intraperitoneally twice weekly, was begun on day 10 or 18. Rats were sacrificed at day 21, 2–4 h after the last drug administration. The severity of arthritis was determined by measuring paw volume using a plethysmometer, visual scoring and histology. Serum was collected for measurement of cytokine levels by ELISA (Biosource International).

LPS-Induced Acute Inflammation

Animals used were rats (male Lewis, 225–250 g, Harlan, Indianapolis, Ind., USA) and monkeys (female cynomolgus, 4–7 years old, 3.2–3.5 kg, Charles River Laboratories, Houston, Tex., USA). Human subjects were in a phase 1 clinical trial. Animals were fasted for 18 h before dosing and humans were fasted overnight, always with free access to water. Vehicle consisted of 1 ml 0.5% methylcellulose-0.025% Tween-20 for rats and 1 ml 0.5% methylcellulose-0.1% Tween-80 for monkeys, both administered intragastrically. Humans received identical capsules for dosing and placebo with about 240 ml of water. Rats were dosed 4 h, monkeys 2 h, and humans 1 h prior to LPS challenge. Rats were dosed at 0, 0.1, 0.3, 1 and 5 mg/kg, and monkeys at 0, 0.3, and 3 mg/kg. Human phase 1 clinical trial doses were fixed at 1, 3, 10, 30 and 100 mg, and placebo, with milligrams/kilogram dosing projected based on an approximation of 70 kg body mass per subject. Intravenous administration of LPS *(E. coli)* was 1 mg/kg for rats, 10 μg/kg for monkeys, and 2 ng/kg for humans. LPS challenge produced a transient elevation of TNFα in plasma that peaked 1–2 h after challenge in rats, at about 1 h in cynomolgus monkeys, and around 2 h in humans. The extent of TNFα inhibition was determined by quantifying plasma TNFα levels by ELISA of treated and untreated plasma from blood collected at various time points and frozen for later assay. Human plasma was also assayed for IL-6. SD0006 plasma exposure was determined by a liquid chromatographic/tandem mass spectrometric (LC-MS/MS) method. The free fraction (FF) for SD0006 was the portion not bound to plasma proteins, and was determined to be 28% for rats and monkeys, and 16% for humans (data not shown).

Immunoblot Analysis

Proteins were separated by sodium dodecyl sulfate polyacrylamide gel electrophoresis and transferred onto nitrocellulose membranes (Invitrogen, Carlsbad, Calif., USA). Membranes were blocked for 2 h at room temperature in 5% nonfat dry milk in PBS with 0.1% Tween-20, and then incubated overnight at 4°C with various antibodies. Antigen-antibody complexes were visualized by incubation of the blots in a dilution of horseradish-peroxidase-conjugated antibodies and the Pierce ECL detection system (Rockford, Ill., USA).

p38 Kinase Isoform Determination

Cell lysates were subjected to immunoblot analysis using polyclonal antibodies unique to the α-, β-, γ-, and δ-isoforms. Though the p38α-specific antibody has slight cross-reactivity with p38β, no p38β was detected by the β-specific antibody in monocytes or fibroblasts. Recombinants for all 4 isoforms were included to demonstrate specificity.

Preparing Lysates

For HWB, 200 μl frozen samples were thawed directly into 3 volumes of ice-cold lysis buffer consisting of 20 mmol/l Tris-HCl (pH 7.5), 150 mmol/l NaCl, 1% Triton X-100, 10% w/v glycerol, 50 mmol/l NaF, 1 mmol/l β-glycerol-phosphate, 1 mmol/l sodium vanadate, 1 mmol/l PMSF, phosphatase inhibitor cocktail I (Sigma), and Complete Protease Inhibitor cocktail (Roche, Basel, Switzerland). They were vortexed and transferred to QiaShredder tubes (Qiagen, Valencia, Calif., USA) for centrifugation at 13,000 *g,* 4°C for 5 min, rinsed with 200 μl more of the lysis buffer, and the process repeated. The supernatant of the combined pass-through was used for assay. For U937 and human monocytes, the same lysis buffer was used, but in lieu of lysis with a Qiashredder, micrococcal nuclease (50 μg/ml; Worthington Biochemicals, Freehold, N.J., USA) and trituration were used. Lysates were subsequently digested in lysis buffer supplemented with RNase (4,000 U/ml; Worthington) and DNase (1 mg/ml; Worthington). The same was done for RASFs using 300 μl of lysis buffer per well after the medium was removed.

Quantifying p38α Activity

p38α activity can be determined by either measuring the phosphorylation level of its substrate, MK-2 (on residues Thr 222 and Thr 334; MK-2 activity is proportional to its phosphorylation by p38α), or that of the substrate for MK-2, Hsp27 (on residues Ser 78 or Ser 82).

Hsp27 Approaches

ELISA for Hsp27 phosphorylation was achieved by either electrochemiluminescence (Meso Scale Discovery, Gaithersburg, Md., USA) using kits with Ser 82 specific and total Hsp27 antibodies (to normalize phosphorylation levels) as per the manufacturer's directions, or by time-resolved fluorescence using the Dissociation-Enhanced Lanthanide Fluorescent Immunoassay (DELFIA; Perkin Elmer, Waltham, Mass., USA). Briefly, 96-well DELFIA plates were precoated with 1 pmol/well of rabbit anti-Ser 82 Hsp27 antibody, washed, sample or standard was added per well for 1 h at 4°C, incubated and washed again, then 10 nmol/l Europium-chelated detection antibody to total Hsp27 was added and shaken for 1 h at 4°C in the dark. After washing again, enhancement solution was added to release the Europium from the chelate, and the plate was read in an instrument set for time-resolved fluorescence, using a Europium 400 nm filter. All materials, solutions, and the Europium conjugation were from Perkin Elmer except for the capture and detection antibodies. The immunoblot approach was as described below.

MK-2 Activity Assay Approach

The same DELFIA plates were precoated as above but with 0.5 pmol of antibodies against Thr 222 and Thr 334 of MK-2 per well, then washed, sample or standard added as above, and washed again. Then 100 μl/well of reaction mixture (5.15 mmol/l $MgCl_2$, 1 μmol/l ATP, 250 nmol/l biotin-Hsp peptide, 20 mmol/l 3-(N-morpholino)-propanesulfonic acid buffer (pH 7.2), 25 mmol/l β-glycerophosphate, 5 mmol/l ethylene glycol-bis(β-aminoethyl ether)-N,N,N′,N′-tetra acetic acid, plus the same phosphatase and protease inhibitors as in the lysis buffer above) was added and incubated in a shaker at 30°C for a time period from 1 to several hours, depending on the amount of activity estimated to be present. For radiolabeling, γ-phosphate ^{33}P ATP with a specific activity of 3,000 Ci/mmol was spiked into the reaction mixture at 50 μCi/ml. At the designated time, well contents were transferred to the corresponding wells on a 96-well streptavidin-coated flashplate (Perkin Elmer). The flashplate was incubated, washed, and labeled peptide quantitated in a scintillation counter.

Quantitating ERK and JNK Activity

ELISA kits specific for phospho-ERK, phospho-JNK, and phospho-cJun were used as per the manufacturer's directions (Meso Scale Discovery).

Determination of SD0006 Concentration in Plasma

SD0006 was quantitated using a solid-phase extraction method followed by injection onto an LC-MS/MS system. SD0006 and its deuterated internal standard were prepared by spiking stock solutions in methanol into normal plasma. Serial dilutions were used to achieve a 9-point standard curve. SD0006 was extracted from plasma, or standard in normal plasma, by loading 25 μl of plasma onto a Waters® (Milford, Mass., USA) Oasis HLB 96-well solid-phase extraction plate, adding 600 μl of analytical internal standard solution standard, washing with 400 μl of 30% methanol in water, and eluting with 150 μl of 85% methanol in 20 mmol/l ammonium acetate buffer into a deep-well collection plate. A 25-μl volume of each extracted sample was introduced into the LC-MS/MS system using a Zorbax Eclipse XDB-C8, 12.5 × 2.1 mm precolumn and Zorbax Eclipse XDB-C8, 50 × 2.1 mm, 5μm particle size, column (MAC-MOD Analytical Inc., Chadds Ford, Pa., USA) and a 60% methanol in 20 mmol/l ammonium acetate buffer mobile phase at 0.25 ml/min. An API 4000 Sciex Mass Spectrometer (Applied Biosystems, Foster City, Calif., USA) with Turbo V interface with an ESI probe was operated in the multiple reaction-monitoring mode to detect SD0006 and the internal standard in the samples. Linear regression analysis from the standards was used to determine the concentration of SD0006 in the plasma samples.

Determination of SD0006 Plasma Protein Binding

The extent of binding of SD0006 to human, rat, and monkey plasma was determined in vitro using an ultracentrifugation method. Each matrix was fortified with SD0006 to achieve concentrations in the projected therapeutic concentration range (from 0.1 to 100 μg/ml). For each concentration, duplicate 4-ml aliquots of plasma fortified with SD0006 were placed in ultracentrifugation tubes and then equilibrated in a water bath maintained at 37°C for 1 h. The tubes were centrifuged in a 37°C centrifuge using a 70Ti rotor (Beckman, Palo Alto, Calif., USA) for 15 h at 150,000 *g*. After centrifugation, a 0.5-ml aliquot of supernatant was removed from the top of each tube. Concentrations were determined in plasma or supernatant by adding 100-μl aliquots of each sample in duplicate to a 96-well plate. The samples were acidified with 300 μl of 0.033 mol/l phosphoric acid containing analytical internal standard. The acidified samples were placed on a 96-well Isolute C18 solid-phase extraction plate (Biotage, Charlottesville, Va., USA) that was previously conditioned with methanol and 0.1% formic acid. The extracts were washed with 5% methanol and 0.1% formic acid prior to elution with acetonitrile. The extracts were evaporated to dryness under nitrogen and resolubilized with mobile phase. The analyte and internal standard were quantitated in the multiple reaction-monitoring mode on an API 4000 LC-MS/MS using peak area ratios. The fraction of SD0006 bound to plasma (F_b) at a given concentration was determined using the following equation:

$$F_b = (C_{total} - C_u)/C_{total}$$

where C_u is the drug concentration recovered in the protein-free supernatant level and C_{total} is the total drug concentration in plasma. The FF equals 1 – Fb.

The FF for SD0006 was determined to be 0.16 for HWB and 0.28 for rat and cynomolgus monkey blood. Ex vivo HWB assays were also corrected for a whole blood/plasma partition ratio of 0.57.

Radiography and Bone Mineral Density

Radiographic images were obtained by exposing hind paws to X-rays at 26 kV for 3 s using a Faxitron radiographic inspection unit with digital camera model MX20/DC2 (Faxitron, Wheeling, Ill., USA). Paws were stored at –80°C until ready for use. Bone mineral density was determined by peripheral quantitative computed tomography using a Norland XCT Research M densitometer (Norland Medical Systems, White Plains, N.Y., USA). Hind paws were removed and frozen pending the analysis. The paws were laid out on the lateral side and 3 serial 1-mm sections were taken beginning 3 mm distal from the tip of the tibia that includes the talus, calcaneous and tarsus bones. Voxel size was 0.09 mm, the analysis was done with the threshold set at 620 mg/cm^3, and trabecular bone area was 99%. Total bone density and total bone area were recorded. The densitometer was calibrated daily with a bone phantom, with a variance less than 2%.

TaqMan One-Step Reverse Transcriptase-Polymerase Chain Reaction Analysis

Rat paws, frozen in liquid nitrogen and stored at –80°C, were precrushed in stainless steel crushers chilled at –80°C and transferred to freezer mill grinding vials. Tissues were ground in a CertiPrep 6750 freezer mill (SPEX CertiPrep, Inc., Metuchen, N.J., USA) according to manufacturer's instructions by doing 2 rounds, each with a 2-min prechill and grinding for 0.4 min. The rat paw powder was then stored at –80°C. RNA was extracted from 300–400 mg powder using the Totally RNA Isolation Kit (Ambion Inc., Austin, Tex., USA). All RNA was further purified by DNase digestion to remove genomic DNA and LiCl precipitation to remove carbohydrates as follows. RNA (100 μg) was precipitated overnight at –20°C by adding 0.5 vol of 7.5 mol/l LiCl/50 mmol/l ethylene diamine tetraacetic acid solution (Ambion Inc.) followed by centrifugation for 30 min at 13,000 *g* at 4°C. The RNA pellet was then resuspended in DNase/RNase-free water, DNase treated using the Qiagen RNase-free DNase kit according to manufacturer's instructions (Qiagen), and quantified.

Primers and probes for TaqMan analysis were designed using Primer Express Software (Applied Biosystems). Probes were synthesized with the reporter dye 6-carboxyfluorescein at the 5′-end and at the 3′-end with a minor groove binder nonfluorescent quencher (MGB-NFQ, except COX-2 with 6-carboxy-N,N,N′,N′-tetramethylrhodamine) (Applied Biosystems). TaqMan reactions were performed using One-Step RT-PCR reagent (Applied Biosystems), 100 ng total RNA, 500 nmol/l each of forward (FP) and reverse (RP) primers and 100 nmol/l probe. 384-well TaqMan plates were used in a BioMek 2000 robot (Beckman Coulter, Fullerton, Calif., USA) and TaqMan analysis was performed using the 7900HT Sequence Detection System (Applied Biosystems). TaqMan cycling conditions were 48°C for 30 min, 95°C for 10 min, followed by 40 cycles of 95°C for 15 s and 60°C for 1 min. Resulting data were analyzed and relative transcription levels calculated using SDS Calculator software (in-house proprietary software) using normal rat paws as the comparator group. Sequences of the rat primers (FP and RP) and probes used in the reactions were as follows; TNFα, for FP = CCGGTTTGCCATTTCATACC, RP = TCCTTAGGGCAAGGGCTCTT, probe = AAAGTCAGCCTCCTCTC; IL-1β, FP = AGGAAGGCAGTGTCACTCATTGT, RP = CTTGGGTCCTCATCCTGGAA, probe = CAGCTACCTATGTCTTGC; IL-6, FP = ATATGTTCTCAGGGAGATCTTGGAA, RP = GTGCATCATCGCTGTTCATACA, probe = AGTTGTGCAATGGCA; COX-2, FP = TCAAAGACACTCAGGTAGACATGATCT, RP = CGGCACCAGACCAAAGACTT, probe = CACGTCCCTGAGCACCTGCGG; MMP-3, FP = TCCCAGGAAAATAGCTGAGAACTT, RP = GAAACCCAAATGCTTCAAAGACA, probe = CCAGGCATTGGCAC; MMP-9, FP = CACTACCAAGACAAGGCCTATTTCT, RP = TCACCCGGTTGTGGAAACTC, probe = CCATGACAAATACTTCTG; MMP-13, FP = TGCACCCTCAGCAGGTTGA, RP = ACATGAGGTCTCGGGATGGAT, probe = TTGGCCAGAACTTC; RANKL, FP = CGTGCAAAGGGAATTACAACAC, RP = AACCTTCCATCATAGCTGGAACTC, probe = CACAGCGCTTCTCA; p38α, FP = CCATCATTCACGCCAAAAGG, RP = TCACATTCTCGTGCTTCATGTG, probe = TCAGCAGCCGCAGCTCCCTGT; MK-2, FP = GCCAAGGAAACCACCAGTCA, RP = CGGAGCCACATAGTACGGTGTA, probe = AACTCTTTGACCACTCCGT; tartrate-resistant phosphatase, FP = GCGGCATCAACGAAAGGT, RP = CAGAGAGTCCTCAGATCCATAGT, probe = CAACGGCTACCTACGC; intercellular adhesion molecule-1 (ICAM), FP = CGGGATGGTGAAGTCTGTCAA, RP = GTGCACGTCCCTGGTGATACT; probe = TGCCTTTAGCTCCCGTGG; monocyte chemotactic protein 1 (MCP-1), FP = CTGTGCTGACCCCAATAAGGA, RP = ACTTGGTTCTGGTCCAGTTTTCTAA, probe = TGGGTCCAGAAGTAC; iNOS, FP = AGCGGCTCCATGACTCTCA, RP = TGCACCCAAACACCAAGGT, probe = ATGCGGCCTCCTTTGAGCCCTCT; IκB kinase1 (IKK), FP = CCTGAAGATCGCCTGTAGCAA, RP = AGTCGAGACACATTCATGCTATCTG, probe = TCCGGTGAGTGGAAG; inducible IKK (IKKi), FP = CACGGACAGCCCTCCTCTT, RP = CTCCACTGCTGAGCCTTTCAG, probe = CTCAGTAGCAGCCTGG; IL-18, FP = CGCCTGTGTTCGAGGACAT, RP = ATTATCAGTCTGGTCTGGGATTCG, probe = TATCGACCGAACAGCCA; Tpl2, FP = AAGCCATCAGATGTGGAAATCCA, RP = TGGACAGTGTCGCCCCATA, probe = ACATTGCCGAGTTATAC; vascular cell adhesion molecule (VCAM), FP = GAAGCCGGTCATGGTCAAGT, RP = GGTCACCCTTGAACAGTTCTATCTC, probe = TGGCTCCTGATGTTTACCCAATTGACAGA.

In vitro Selectivity Assays

The selectivities of DAPs for p38α were tested against a variety of targets. Inhibition studies were carried out using ATP concentrations at the K_m measured for the respective enzymes and substrate concentrations 10-fold greater than the K_m determined for each kinase. However, there was some difference among assays. For instance, p38α and JNK were tested for their DAP sensitivity, which was tested in 10-fold serial dilutions beginning at 200 μmol/l in 10% dimethylsulfoxide. Reactions were initiated by addition of activated p38α (20–40 nmol/l) or JNK (150–300 nmol/l) previously activated with glutathione S-transferase (GST)-MAP kinase kinase 6 (MKK-6) or GST-MKK-7b, respectively. p38α and JNK activities were determined by following the phosphorylation of epidermal growth factor receptor peptide and GST-cJun, respectively. Reaction mixtures included 50-μl reaction volumes containing 10 mmol/l magnesium acetate, 4% glycerol, 0.4% bovine serum albumin, 0.4 mmol/l dithiothreitol, 1 mmol/l Na_3VO_4, 25 mmol/l 4-2-hydroxyethyl-1-piperazineethanesulfonic acid (HEPES), pH 7.5, 50 μmol/l unlabeled ATP, 200 μmol/l epidermal growth factor receptor peptide or 10 μmol/l GST-cJun, and 0.05 to 0.11 μCi (γ-^{33}P) ATP at pH 7.5. Reactions were stopped by addition of 150 μl of Dowex AG 1 × 8 resin in 900 mmol/l sodium formate buffer, pH 3.0. Addition of resin to the reaction resulted in the precipitation of unreacted ^{33}P-ATP and separation from the ^{33}P-labeled substrate due to enzymatic activity. This method allowed kinase activity to be quantified through measurement of ^{33}P-labeled substrate present in an aliquot taken from the reaction supernatant.

Crystallography

A crystal structure of the p38α/inhibitor complex was obtained using SC79659, which differs from SD0006 only by substitution of the pyridine ring with a pyrimidine and gives the same binding conformation. Purified p38α kinase was concentrated to 6 mg/ml in 50 mmol/l HEPES, pH 7.5, 50 mmol/l NaCl, 5% glycerol and 2 mmol/l dithiothreitol and then SC75422 (2-fluoro-4-[4-(4-fluorophenyl)-2-H-pyrazol-3-yl]pyridine) was added to a concentration of 1 mmol/l. The p38α kinase/SC-75422 complex solution was mixed 1:1 with a reservoir solution containing 14–26% PEG 3000, 5–80 mmol/l $CaCl_2$, and 50 mmol/l N-cyclohexyl-2-aminoethanesulfonic acid, pH 9.0 in a Q-plate sitting drop crystallization plate. Prism-shaped crystals grew at ambient temperature to a maximum size of 0.4 × 0.2 × 0.2 mm over a period of 1–2 weeks.

Cocrystals of p38α/SC-75422 were used as 'surrogate native' crystals for soaking experiments. SC75422 (fig. 1) was displaced at the ATP-binding site of p38α kinase by using an excess of SC79659 in the soaking experiments. The p38α kinase/SC75422 cocrystals were stabilized in 24% PEG 3000, 80 mmol/l $CaCl_2$, 50 mmol/l N-cyclohexyl-2-aminoethanesulfonic acid, pH 9.0 and 1 mmol/l of SC79659; soaking experiments were done over a period of at least 24 h at room temperature. These experiments resulted in a unique ternary complex of p38α kinase with two different inhibitors: the weak inhibitor (SC75422) bound at the distal site and the more potent inhibitor (SC79659) bound at the ATP-binding site of the enzyme.

Diffraction data were collected on ADSC Quantum 210 detector, using synchrotron X-rays generated at beamline 17-ID in the facilities of the Industrial Macromolecular Crystallography Association Collaborative Access Team at the Advanced Photon Source (Argonne National Laboratory, Argonne, Ill., USA). A

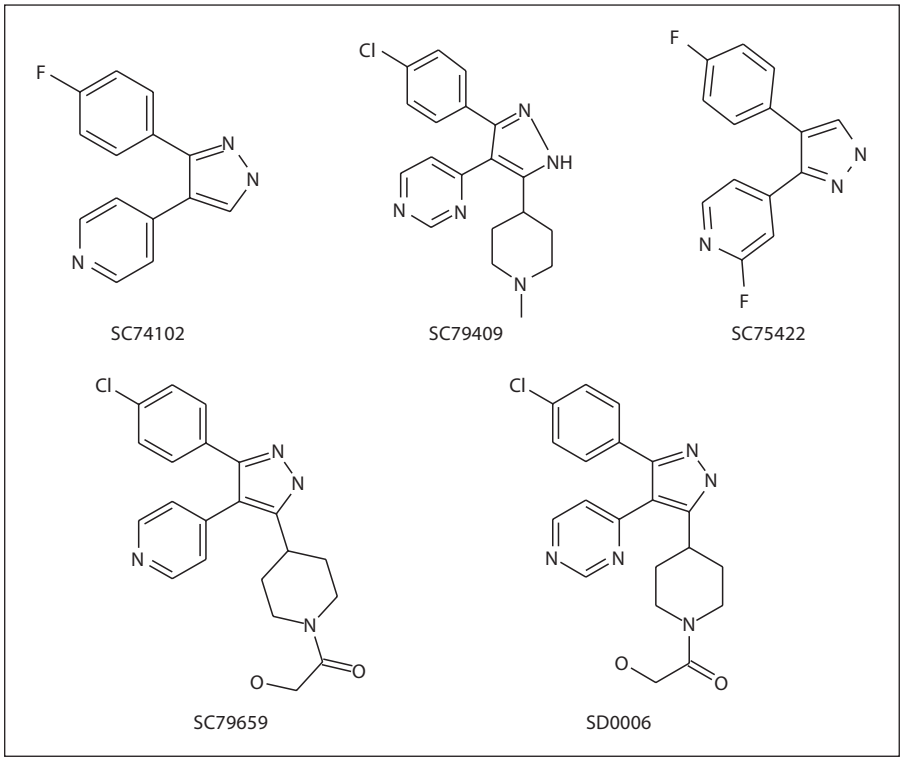

Fig. 1. Structures of 4 DAPs, including SD0006 and the parent compound SC74102, and SC75422 used to create 'surrogate native' crystals.

crystal of the p38α kinase complex with SC79659 was transferred to a small loop from the soak solution cryo-protected with 20% ethylene glycol and flash frozen in a bath of liquid nitrogen. The diffraction data were 99.9% complete with an R_{sym} of 6.5% to 1.98-Å resolution. A total of 24,205 unique reflections were derived from 300 images with a redundancy of 6.5-fold. The crystal belongs to the space group $P2_12_12_1$ with unit cell dimensions a = 64.99 Å, b = 74.65 Å, and c = 77.22 Å. Data reduction and processing were performed with the HKL2000 suite of programs [44].

The crystal structures of the complex were solved by difference Fourier methods using the known structure of p38α kinase, which was derived based on the published structure of ERK-2, a close MAP kinase homologue [45]. Electron density maps were calculated after a few cycles of rigid body, positional and B-factor refinement. Clear, unambiguous electron density was visible for SC79659 at the ATP-binding site and for SC75422 at the distal site. Inhibitors were modeled into the electron density using the program O [46] and further refined using the program X-plor [47]. The structure of the SC79659 complex has been refined to 1.98-Å resolution with R_{work} = 21.5% (R_{free} = 27.2%) with good stereochemistry.

Results

SD0006 Is a Potent, Selective, ATP-Competitive Inhibitor of p38α

SD0006 is the lead compound of 3 DAPs (including SC79409 and SC79659) with a pyridinyl substitution at the 5-pyrazole position of the basic scaffold, represented by the parent compound, SC74102 (fig. 1). The trisubstituted compounds exhibited increased selectivity and some potency over the disubstituted SC74102, and were at least 10-fold selective over all other kinases screened except epidermal growth factor (EGFR) and casein kinase-1δ (CK) (table 1), with greater than 100-fold selectivity based upon IC_{50} ratios over the other MAPKs p38γ, p38δ, ERK-2 and JNK-1, -2, and -3. SD0006 was the most effective in the rat SCW model, had a moderate window against p38β (>40× by IC_{50} ratios; table 1), and became the primary choice for in vivo studies, including a phase 1 clinical trial. Kinetic analyses indicated that these compounds were reversible, non-time-dependent ATP competitive inhibitors, with SD0006 K_i values for p38α and p38β of 61 and 510 nmol/l, respectively (8-fold selectivity ratio based upon Ki ratios; data not shown).

SC79659 differs from SD0006 only by substitution of the pyridine ring with a pyrimidine and gives the same binding conformation. A crystal structure of the p38α/SC79659 complex confirmed that binding was at the ATP binding site of p38α (fig. 2). One edge of the pyrazole moiety was stabilized by interactions with the flexible glycine flap (residues 33–39 that contain the consensus motif, Gly-X-Gly-X-X-Gly), while the central pyrazole

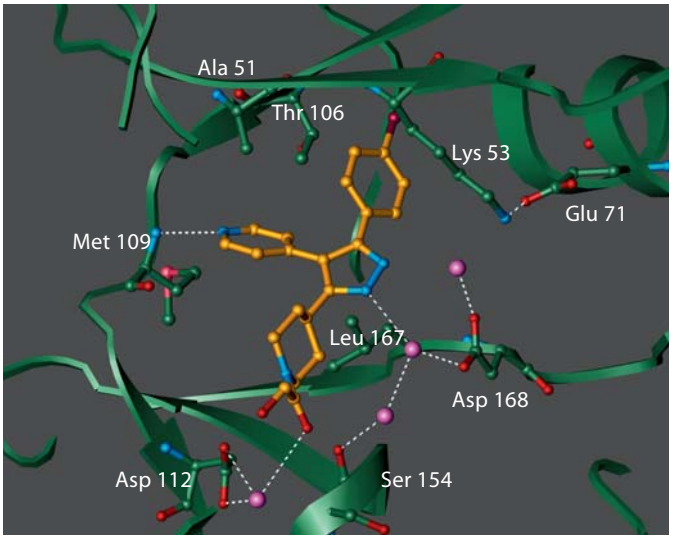

Fig. 2. Crystal structure of p38α/inhibitor complex. Shown is SC79659 (gold, with nitrogen indicated in blue) which differs from SD0006 only by substitution of the pyridine ring with a pyrimidine and gives the same binding conformation. Binding is at the ATP binding site of p38α located at the hinge region between the two lobes of the enzyme. Some of the protein residues that are in close contact with the inhibitor are shown. Also shown are the ordered water molecules (purple spheres). Potential hydrogen bonds are shown in dotted lines. Crystals of p38α complex were obtained, and diffraction data were measured, as described in Materials and Methods. The flexible glycine loop has been omitted for clarity.

formed two water-mediated interactions with Asp168 and Ser154. The pyridine ring forms a hydrogen bond with the peptide nitrogen of Met109. Residues in the glycine flap have been implicated in the binding of the phosphate groups of ATP [48]. The piperidyl group is sandwiched between protein side chain atoms from the glycine loop and the hinge region while the terminal glycolic moiety forms a water-mediated interaction with Asp112. The 4-cholorophenyl group is bound in the lipophilic pocket of the enzyme. It is this interaction that determines most of its potency and selectivity, which is attributed to the presence of the Thr 106 gatekeeper residue. The corresponding residue in most other kinases is too bulky to allow access to the pocket. For example, approximately 40% of kinases in the human kinome contain a methionine residue at this position while 14% of human kinases have a phenylalanine residue at the corresponding position. These data demonstrate that ATP-competitive inhibitors can be selective inhibitors for p38α.

Table 1. Inhibitory activity of DAP p38α inhibitors on various targets

Targets	IC_{50}, μmol/l			
	SC74102	SC79659	SC79409	SD0006
Ab-l	>10	>10	>10	>30
Akt-1	>10	>10	>10	>30
ASK-1				>10
Aur-2			>10	>10
CDC-7			>10	>10
CDK-2	21.1	>100	>200	>30
CHK-1	>10	>10	>10	>30
CK1δ	<1	<1	0.017	0.029
CK2α	>10	>10	>10	>30
EGFR-1	<1	<1	<1	0.101
ERK-2	>100	>100	>100	>200
FGFR-1	>10	>10	>10	>30
GSK3β	>10	>10	>10	>30
IGFR-1			>10	>10
IKK-1	>200	>100	>100	>200
IKK-2	>200	>100	>100	>200
IKKi	>100	>100	>100	>30
IR			>10	>10
JNK-1	21.5	59.4	>200	>50
JNK-2	1.35	2.75	19.7	9.7
JNK-3	3.67	1.85	69.7	>3.1
Kit			>10	
Lck	>10	>10	>30	>30
Lyn		2.0	>10	>10
MAPKAP-K2	>10	>10	>200	>200
Met	>10	>10	>10	>30
MK-3	>100	>100	>200	>200
MKK-1				>10
MKK-6				>10
MKK-7				>10
MNK	6.42	>100	>200	>200
MSK			>200	>200
Nim			>10	>10
p38α	0.382	0.111	0.048	0.016
p38β	5.08	1.79	2.32	0.677
p38γ	>100	>100	>100	>100
p38δ	>100	>100	>100	>100
PAK-4	>10	>10	>10	>30
PDGFR			>10	>10
PDK-1	>10	>10	>10	>30
PKA	<10	>10	10.5	3.69
PKCα			>40	
PKCβ	>10	>10	>10	23.5
PKCζ	>10	>10	>30	>29
PLK-1			>10	>10
PRAK	>100	>100	>200	>200
Ret			>10	>10
RSK-2	40.7	>100	>100	
RSKb			>200	199
STLK-2			>10	>10
SULU			>10	>10
TBK-1	>100	>100	>100	
TRKA	>10	>10	>10	>30
VEGFR-2	>10	>10	>10	>10
VEGFR-3			>10	>10
ZAP-70		>10	>10	>10
COX-1	>100	>10	>500	>100
COX-2	>100	>10	>500	>100

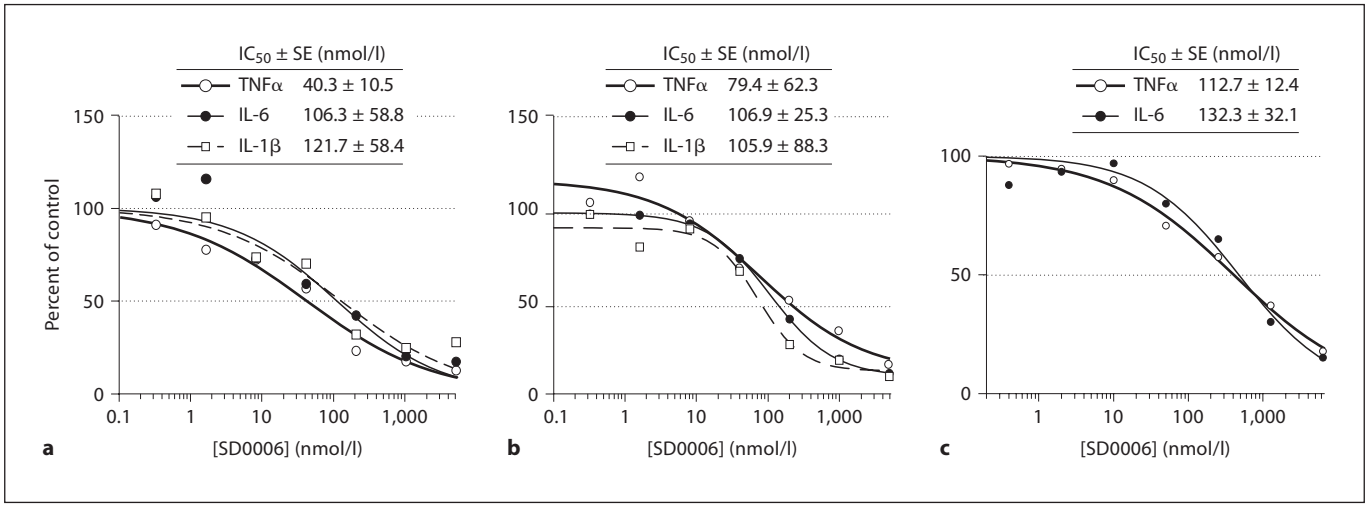

Fig. 3. Ex vivo equivalence of inhibition by SD0006 of inflammatory cytokine release in LPS-challenged U937 cells (**a**), human primary monocytes (**b**), and HWB (**c**). Cells were preincubated with SD0006 for 60 min, challenged with LPS, then medium or plasma was collected to determine cytokine release as a mechanism biomarker (after 4 h for TNFα and IL-6 and 16 h for IL-1β, for all cell types, except 16 h for IL-6 from U937 cells). Data are averages from 3 donors for monocytes, 6 donors for HWB, and 2 assays for U937 cells. Curve fit, IC_{50} determinations, and standard errors (SEs) were made using Grafit 5(2) software, with HWB values corrected for the FF in plasma.

SD0006 Suppresses Inflammatory Mediator Release in Cellular Studies

Since macrophages, monocytes and fibroblasts are key players in RA synovium and produce most of the inflammatory mediators in RA disease, we utilized representative cell-based assays consisting of primary human monocytes, a human monocytic cell line (U937, differentiated by phorbol ester into a macrophage phenotype), and RASFs. Using phospho-specific antibodies to each of the 4 p38 kinase isoforms, we verified that p38α was predominant in all cell types (data not shown). The related MAPKs, ERK-1 and ERK-2, and JNK-1 and JNK-2, were also detected in all 3 cell types. We also used WB to represent the physiological in vivo milieu.

Since p38α, JNK and ERK were present in primary monocytes, and consequently in human blood, and also in monocytically derived U937 cells, these cell types were used to determine the degree to which inflammatory cytokine production could be blocked by selective p38α inhibition. Figure 3 shows that treatment with SD0006 gave dose-dependent and near-total blockade of LPS-induced TNFα release with very comparable IC_{50}s in U937 cells (fig. 3a) as well as for both primary monocytes (fig. 3b) and HWB (fig. 3c) (with HWB corrected for plasma protein binding and whole blood/plasma partition factors). SD0006 also suppressed IL-1β and IL-6 production with IC_{50}s very comparable from either U937 cells (fig. 3a), or primary monocytes (fig. 3b), and also for IL-6 from HWB (fig. 3c). In fact, all 3 cytokines from all 3 cell assay types had IC_{50}s that were very close to one another. Results are summarized in table 2. These data demonstrate that selective pharmacological modulation of p38α is sufficient to suppress inflammatory cytokine production by monocytic cells.

RASFs were used to evaluate the role of p38α in the regulation of IL-1β induced COX-2 expression and PGE_2 release. SD0006 has no direct inhibitory activity against COX-1 or COX-2 (table 1), yet it could completely inhibit in a dose-dependent manner the release of IL-1β-stimulated PGE_2 with an IC_{50} of 96.2 nmol/l (fig. 4a). The mechanism was via the selective blockade of COX-2 protein expression (COX-1 was unaffected; fig. 4b). Suppression of COX-2 expression was not due to cytotoxicity since by the 3-(4,5-dimethylthiazol-2-yl)-2,5-diphenyltetrazolium assay, there was no significant effect at the highest concentrations evaluated (data not shown).

The p38α, ERK and JNK pathways are all activated by IL-1β in RASFs. SD0006 clearly inhibits p38α as shown by the dose-dependent inhibition of phosphorylation of its endogenous Hsp27 substrate in figure 5a. The activation of p38α itself was suppressed, though SD0006 does not seem to inhibit MKKs directly (table 1), an effect that has been previously reported for other p38 kinase inhibitors [49] (fig. 5b). However, ERK and JNK pathways were not inhibited by SD0006, which underscores the importance

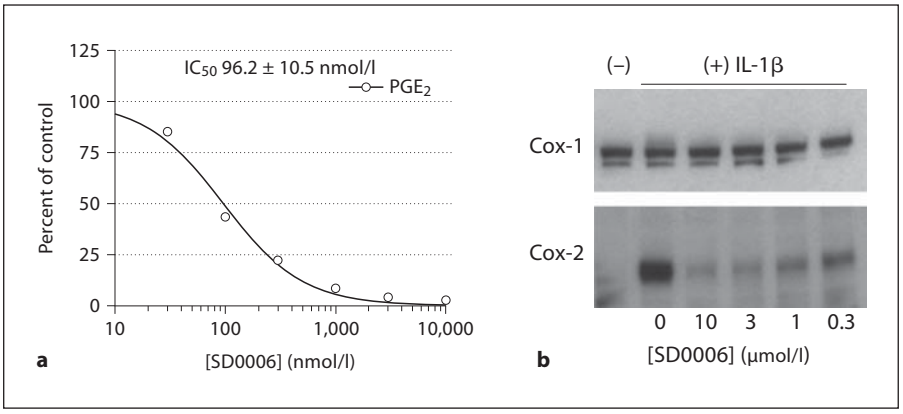

Fig. 4. Concentration-dependent inhibition of COX-2 protein expression and PGE_2 release by SD0006 in a human RASF cell line in response to IL-1β. **a** Dose-dependent inhibition of PGE_2 release. IC_{50} determinations were made using Grafit 5(2) software with data from two experiments. Inhibitor was added 1 h before stimulation with 1 ng/ml IL-1β, then after 20 h supernatants were removed and assayed for PGE_2 as described in Materials and Methods. **b** Western blots demonstrating selective inhibition of COX-2 protein expression compared with COX-1. Cells were treated as in **a** but collected after 4 h of stimulation.

Table 2. Anti-inflammatory efficacy of SD0006

Cytokine release from LPS-challenged:	TNFα	IL-6	IL-1β	p38
U937 cells (IC_{50}, μmol/l)	0.040	0.106	0.122	
Primary human monocytes (IC_{50}, μmol/l)	0.079	0.107	0.106	0.047* to 0.058**
HWB ex vivo (IC_{50}, μmol/l)	0.402	0.471		
HWB ex vivo (IC_{50}, μmol/l, FF)	0.113	0.132		
Humans (clinical trial)				
HWB in vivo (ED_{50}, mg)	11.3			
HWB in vivo (EC_{50}, μmol/l)	0.316	0.248		
HWB in vivo (EC_{50}, μmol/l, FF)	0.051	0.040		0.036**
Cynomolgus monkey				
Percent inhibition	80% at 0.3 mg/kg			
ED_{50}, mg/kg	0.104			
EC_{50}, μmol/l, FF	0.036			
Rats				
Percent inhibition	87% at 5 mg/kg			
ED_{50}, mg/kg	0.30			
EC_{50}, μmol/l, FF	0.058			
Mice				
Percent inhibition	91% at 10 mg/kg			
Other determinations:				
PGE_2 release from IL-1β-stimulated RASF cells (IC_{50}, μmol/l)	0.092			
Rat SCW paw swelling				
ED_{50}, mg/kg	1.51			
EC_{50}, μmol/l, FF	0.48			

* By MK-2 activity assay; ** by Hsp27 phosphorylation assay.

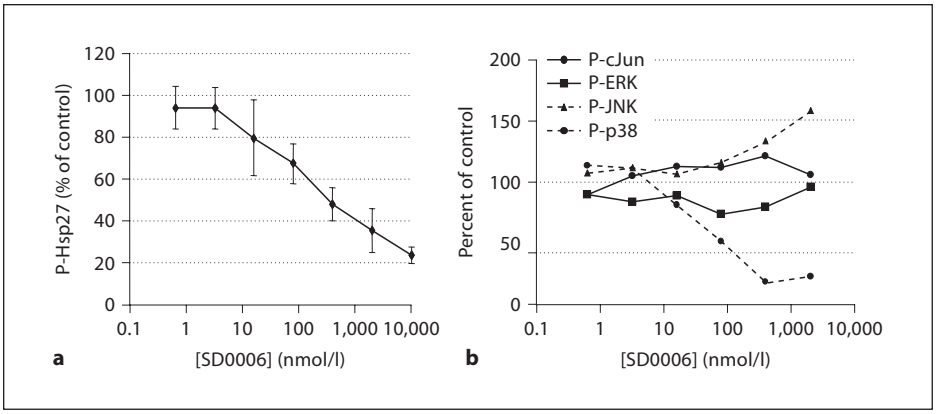

Fig. 5. Inhibition by SD0006 in RASFs of p38 kinase activation and activity, but not of ERK or JNK. RASF cells were preincubated with inhibitor for 60 min, then challenged with human recombinant IL-1β (1 ng/ml, 30 min) as described in Materials and Methods. **a** Phosphorylation of Hsp27 was determined by subjecting lysates to Western blotting with phospho-specific antibodies, followed by densitometry. Error bars are the standard deviation for 3 assays. **b** Activation states of p38, ERK, JNK, and phosphorylation of the JNK substrate, cJun, were determined by subjecting lysates to electrochemiluminescence-based ELISAs as described in Materials and Methods. Data shown are the average values of 2 assays.

Table 3. Amelioration of disease severity in animal models by SD0006

	Improvement relative to control
Rat carageenan paw(30 mpk)	67% pain 58% paw swelling
Rat SCW arthritis	95.1% at 60 mg/kg 43.7% at 2 mg/kg
Mouse CIA	16% incidence at 15 mg/kg b.i.d. vs. 89% in vehicle control

of p38α in IL-1β-mediated signal transduction (fig. 5b). Figure 5b also illustrates that SD0006 did not enhance the activation of ERK, and had only a small effect at high concentrations upon enhancing the activation of JNK, as has been reported for other p38α inhibitors [50, 51]. These results show that selective pharmacological modulation of p38α is sufficient to suppress inflammatory COX-2 and PGE_2 production by synovial fibroblasts.

SD0006 Alleviates Swelling and Pain in a Rodent Acute Inflammation Model

The effectiveness of DAPs in vitro for downregulating COX-2 and PGE_2 production led to an evaluation in the rat carrageenan paw inflammation model, in which inflammation and pain have been shown to be dependent upon upregulation of COX-2 because selective inhibitors of COX-2 markedly reduce both responses [52]. Figure 6 shows that SD0006 was equally effective at 30 mg/kg as an analgesic whether given prophylactically (2 h before, fig. 6a) or therapeutically (3 h after, fig. 6b) carageenan injection, with 67 and 61% pain reduction, respectively (by Hargreave's hyperalgesia model). This tracked well prophylactically with reduction in paw swelling (58%), and therapeutically was equally efficacious as dexamethasone (70% pain reduction) for analgesia (table 3). Results were consistent with the ability of SD0006 to suppress PGE_2 production in vitro (fig. 4b). These data indicate that selective pharmacological modulation of p38α can have analgesic benefit in acute inflammation.

SD0006 Is Effective in Mouse Collagen-Induced Arthritis

Mouse collagen-induced arthritis (CIA) is an attractive disease model because the histopathology of CIA joint inflammation is similar to that of human RA. As in human RA, mice respond to methotrexate, dexamethasone, and biological therapy (using antibodies to TNFα and IL-1β) [53]. SD0006 dose-dependently reduced disease incidence by 82% relative to the vehicle control (fig. 7; table 3), an effect that was equivalent to anti-TNFα antibody treatment. These data suggest that orally available inhibitors of p38α may be an effective alternative to steroids and biologics for RA therapy.

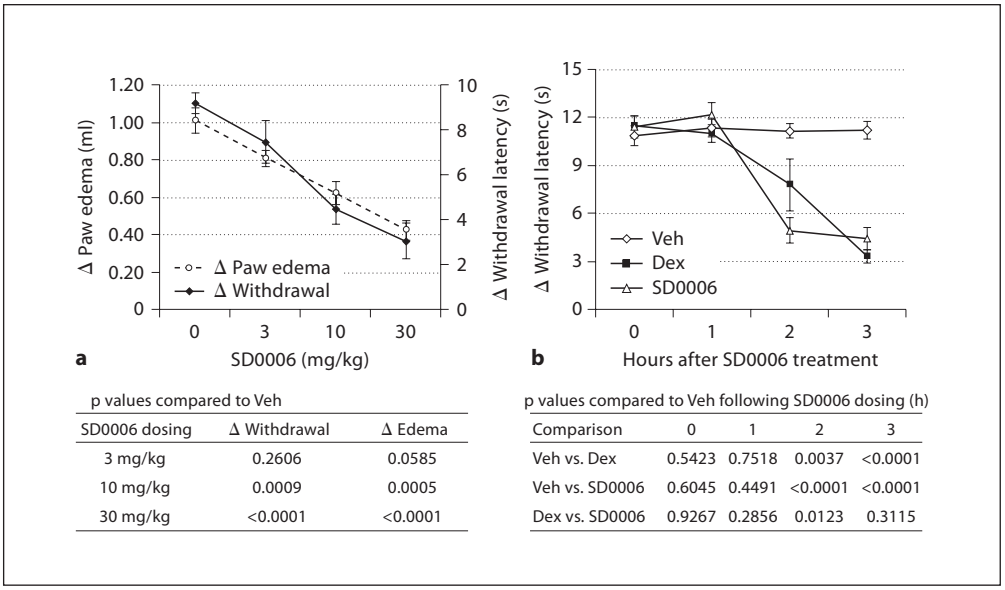

p values compared to Veh

SD0006 dosing	Δ Withdrawal	Δ Edema
3 mg/kg	0.2606	0.0585
10 mg/kg	0.0009	0.0005
30 mg/kg	<0.0001	<0.0001

p values compared to Veh following SD0006 dosing (h)

Comparison	0	1	2	3
Veh vs. Dex	0.5423	0.7518	0.0037	<0.0001
Veh vs. SD0006	0.6045	0.4491	<0.0001	<0.0001
Dex vs. SD0006	0.9267	0.2856	0.0123	0.3115

Fig. 6. In the carrageenan rat paw model, SD0006 reduces pain and swelling prophylactically (**a**) and therapeutically reduces pain with efficacy equal to steroids (**b**). **a**, **b** The data represent the means ± SEM based on 5 rats per group. Procedures and quantification of responses were as described in Materials and Methods. Veh = Vehicle; Dex = dexamethasone. **a** Hyperalgesia (pain; determined by change in paw withdrawal latency time) and edema (paw swelling; determined by change in paw volume) dose-response to pretreatment dosed 2 h before carrageenan injection and measured 3 h after for response. One-way analysis of variance (ANOVA) on the hyperalgesia and edema data from the SD0006 dose-response study was performed separately and then each dose group was compared to the vehicle control using Dunnett's t test, and the p values from the pairwise comparisons are shown. The 10 mg/kg and 30 mg/kg SD0006 dosings were statistically highly significant compared to controls for both readouts at the 5% significance level. **b** Hyperalgesia therapeutic response compared to steroid. Vehicle (0 mg/kg), SD0006 (30 mg/kg), or dexamethasone (3 mg/kg) were administered orally 3 h after carrageenan injection, and pain was measured 1, 2, and 3 h afterwards. A repeated analysis of variance model was utilized on the longitudinal data set of the change in withdrawal latency times considering that measurements from the same animal are correlated. Based on results of the repeated analysis of variance, at 2 and 3 h posttreatment both dexamethasone and SD0006 were strongly significantly different from vehicle control at the 5% test level. Also, at the 2-hour time point, SD0006 was significantly different from dexamethasone. p values of the comparisons at the posttreatment hours are shown.

SD0006 Attenuates SCW-Induced Inflammation and Bone Loss

Arthritic response in the SCW model is biphasic, characterized by an acute phase after SCW injection from day 1 to 5 (fibrin and hemorrhage in the synovium, activated macrophages in the soft tissue, and mild osteolysis), followed by a chronic joint erosion stage from days 10 to 28 (intense cell infiltration, inflammation, and bone destruction). A role for TNFα and IL-1β has also been demonstrated in the chronic phase of this model by the therapeutic role of biologics with neutralizing antibodies to TNFα and IL-1β [54, 55] [J. Monahan, unpubl. obs.]. SD0006 was found to inhibit the transcription of several inflammatory mediators to prevent joint swelling and bone destruction and to preserve bone density.

Because TNFα signaling modulates the expression of many genes induced by SCW, and has been reported to

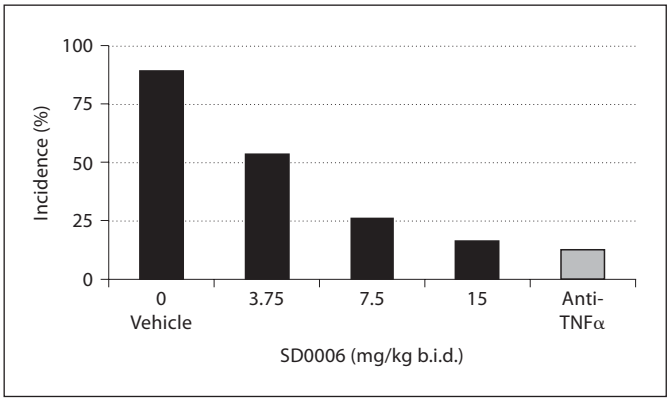

Fig. 7. Dose-dependent reduction in the incidence of arthritis by SD0006 in the mouse CIA model is equivalent to anti-TNFα treatment. Mice were treated from day 21 to 56 with either anti-murine TNFα antibody (n = 70) or SD0006 at the indicated doses (n = 19 per dose), as described in Materials and Methods.

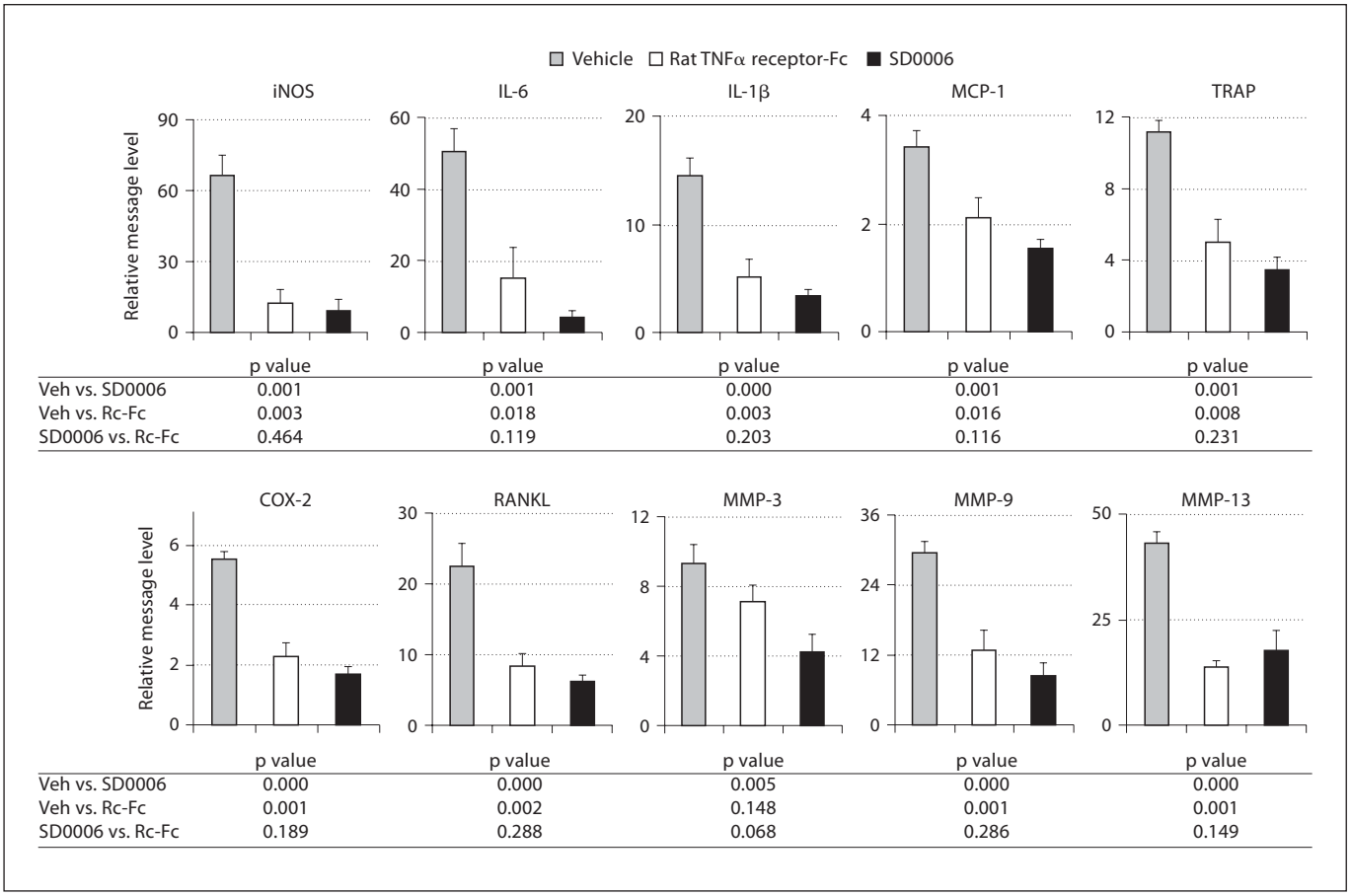

	p value	p value	p value	p value	p value
Veh vs. SD0006	0.001	0.001	0.000	0.001	0.001
Veh vs. Rc-Fc	0.003	0.018	0.003	0.016	0.008
SD0006 vs. Rc-Fc	0.464	0.119	0.203	0.116	0.231

	p value	p value	p value	p value	p value
Veh vs. SD0006	0.000	0.000	0.005	0.000	0.000
Veh vs. Rc-Fc	0.001	0.002	0.148	0.001	0.001
SD0006 vs. Rc-Fc	0.189	0.288	0.068	0.286	0.149

Fig. 8. The transcription of several proinflammatory cytokines in the rat SCW model by SD0006 is inhibited with comparable efficacy to an anti-rat TNFα biologic. Vehicle (Veh) is SCW inoculated transcription relative to normal control. Treated animals (8 per group, including vehicle control) were given 15 mg/kg SD0006 b.i.d. daily from days 18 to 21. On day 21, total RNA was isolated and subjected to TaqMan analysis as described in Materials and Methods. One-way analysis of variance on each mRNA endpoint was performed to compare both the rat biologic and SD0006 therapies to the vehicle control and to each other, with p values of the pairwise comparisons from the analysis of variance shown in the figures. SD0006 was always statistically significantly different from control, as was the anti-rat TNFα biologic for all but MMP-3 at the 5% significance level.

stimulate osteoclastogenesis in synergy with RANKL [56], we used real-time RT-PCR (TaqMan) analysis of paw mRNA to determine SCW arthritis-induced changes in gene expression. To confirm the role of TNFα in the expression of these genes, we evaluated the effects of the sTNFRII-Fc chimera on RNA expression and compared it to that of SD0006. To determine the effects on gene expression of cells that have already infiltrated the joints, treatment was performed from day 18 to day 21 where the disease is quite advanced. IL-6, IL-1β, iNOS, RANKL, COX-2, tartrate-resistant phosphatase (TRAP), MCP-1, and MMP-3, -9, and -13 were all found to be elevated by SCW arthritis, and all were reduced by both SD0006 and sTNFRII-Fc with no significant difference between the two treatments (except for MMP-3 where sTNFRII-Fc was less effective) (fig. 8). Little or no inhibition of transcription was observed for TNFα, IL-18, VCAM and ICAM, p38α, MK-2, IKKi, IKK2, or Tpl2 (data not shown). The lack of effect on TNFα message was not surprising since the main effect of p38α inhibitors on TNFα is known to be at the translational level [21]. Comparable results have been found for SC79409 [57].

SD0006 was also highly effective in attenuating SCW-induced inflammation as shown by the dose-dependent inhibition of paw swelling in figure 9. SD0006 was administered from days 10 to 21, the period where untreat-

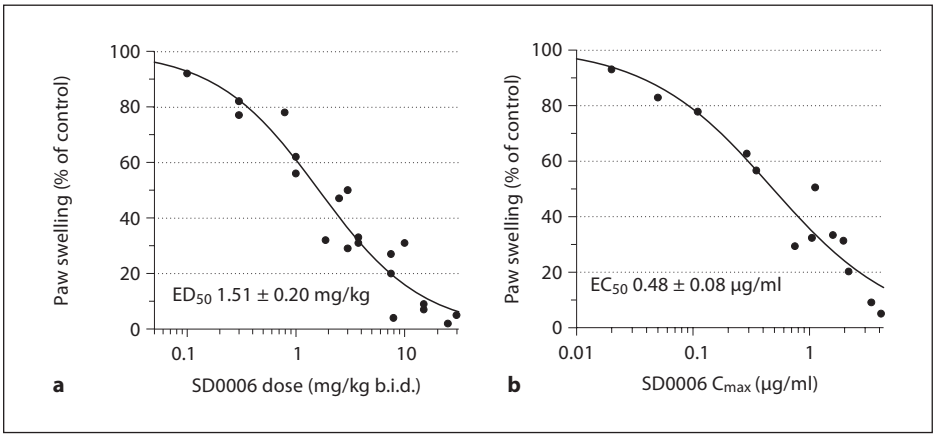

Fig. 9. SD0006 inhibits paw swelling in rat SCW-induced arthritis. SD0006 was administered from days 10 to 21, then plasma was taken from arthritic rats at various times on day 21 and compound levels were determined as described in Materials and Methods. The number of animals per group was between 4 and 8. Two paw volume observations were taken for each animal. C_{max} and AUC were determined from plasmas taken from 3 animals per time point. Inhibition of edema as a function of SD0006 dose (**a**) or C_{max} (**b**) was determined by a 4-parameter logistical model. ED_{50} and EC_{50} determinations were made using Grafit 5(2) software.

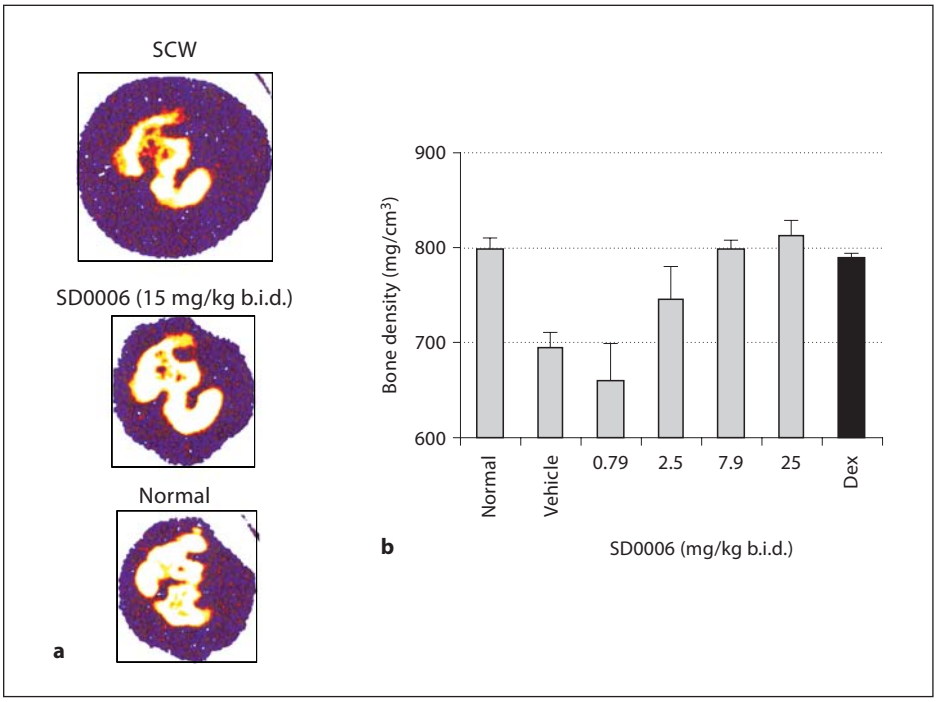

Fig. 10. SD0006 protects against inflammation-mediated joint and bone destruction. Rats were inoculated with SCW and were either left untreated, or were orally given SD0006 b.i.d. 10 days later. Assessment was conducted on day 21. **a** Computed tomographies of paws from SCW-treated rats with 15 mg/kg SD0006 b.i.d. (center) and without (top), as compared to a normal, untreated control paw (bottom). Purple represents soft issue that swells with SCW-induced edema. White represents high-density bone, yellow and red are indicative of decreasing bone density and erosion. **b** Hind paws from rats treated as indicated with SD0006 (4 per group) were analyzed for bone density as described in Material and Methods. Error bars are SEM. Dunnett's t test was utilized to compare the normal control with the drug-dosed groups following a one-way ANOVA overall significant F test of the bone density data. The 7.9- and 25-mg/kg b.i.d. SD0006 dose groups and the dexamethasone (Dex)-treated group were all shown to be statistically indistinguishable from the normal control with p values ≥ 0.994 for the comparisons.

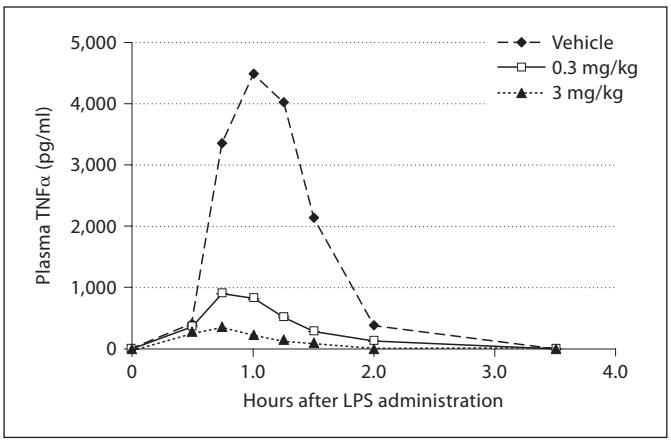

Fig. 11. Time course of LPS-induced TNFα production in cynomolgus monkeys and inhibition by SD0006. Treatment and analyses were as described in Materials and Methods. Values are the mean of 3 samples per treatment group; standard errors were less than 10% of the mean for all sample groups.

ed control rats exhibit profound joint inflammation, and plasma levels were determined following the last dose on day 21. The ED_{50} was found to be 1.51 mg/kg b.i.d. (fig. 9a), and the EC_{50} value for C_{max} was 0.48 μg/ml (fig. 9b). Disease severity was ameliorated 43.7% at 2 mg/kg and 95.1% at 60 mg/kg, b.i.d. (table 3).

Finally, figure 10 demonstrates that p38α signaling is essential to bone destruction in SCW-induced arthritis. Computed tomography cross-sectional scans (fig. 10a) demonstrated that the apparent joint architecture and swelling of paws from SD0006 treated animals was nearly indistinguishable from normal, untreated controls. Measurement of bone mineral density measured by peripheral quantitative computed tomography indicated that it was normalized by SD0006 (fig. 10b), and was comparable to results achieved with dexamethasone. Similar results have been reported for SC79409 [57]. These data demonstrate that selective pharmacological modulation of p38α is sufficient to suppress arthritis and bone erosion in animal disease models with efficacy similar to anti-TNFα biologics.

SD0006 Suppresses TNFα Release in Experimental Endotoxemia

In vivo, the LPS-induced acute inflammation model (experimental endotoxemia) was used to evaluate the oral efficacy and potency of SD0006 as a blocker of TNFα production. In rats, SD0006 induced dose-dependent inhibition of TNFα release with an ED_{50} of 0.30 mg/kg (table 2). Figure 11 shows the SD0006 dose and time response for cynomolgus monkeys, with TNFα release nearly abated at 3 mg/kg. Table 2 gives the SD0006 ED_{50} and EC_{50} results corrected for the plasma FF, which were 0.30 mg/kg and 0.058 μmol/l for rats and 0.104 mg/kg and 0.036 μmol/l for monkeys, respectively. The close agreement between rodent and primate species, especially for the EC_{50} (FF), was very useful for SD0006 dosing projections for humans, the results from a clinical trial being shown in table 2 as well, where the ED_{50} and EC_{50} (FF) results were found to be 11.3 mg and 0.051 μmol/l, respectively. The dose and concentration curves for all 3 species overlapped (fig. 12a, b), providing excellent agreement between preclinical studies and clinical results.

SD0006 Inhibition of p38α Correlates to That of TNFα Release in LPS-Induced Acute Inflammation

Table 2 also summarizes the results of LPS acute inflammation model studies that established a correlation between inhibition of p38α and that of TNFα release. These studies utilized cell-based assays with LPS-challenged primary human monocytes ex vivo, and human clinical studies in vivo. Both in vivo and ex vivo, samples were assayed for p38α activity near the signaling peak following LPS challenge, determined either directly by measuring MK-2 activity (dependent on activation by p38α) or indirectly by measuring Hsp27 phosphorylation (dependent on MK-2 activation). This was compared to TNFα measured in the plasma or media at a later time point.

Ex vivo results are shown for primary human monocytes in figure 13a, where p38α activity as determined by either MK-2 activity assay or by Hsp27 phosphorylation gave overlapping dose-response curves, verifying that either assay could be used to determine p38α activity. The primary monocyte IC_{50}s for p38α and TNFα were 0.058 μmol/l (by Hsp27 phosphorylation) and 0.079 μmol/l, respectively (table 2).

In vivo, inhibition of p38α activity, and TNFα and IL-6 release in humans were parallel at the C_{max} time point with comparable EC_{50}s of 0.036, 0.051, and 0.040 μmol/l, respectively (table 2; fig. 13b). All these data are within an approximately 2-fold range, providing confidence that mechanisms which target modulation of p38α can proportionately control inflammatory mediator release, and are sufficient to suppress inflammatory cytokine production in vivo in acute inflammation models.

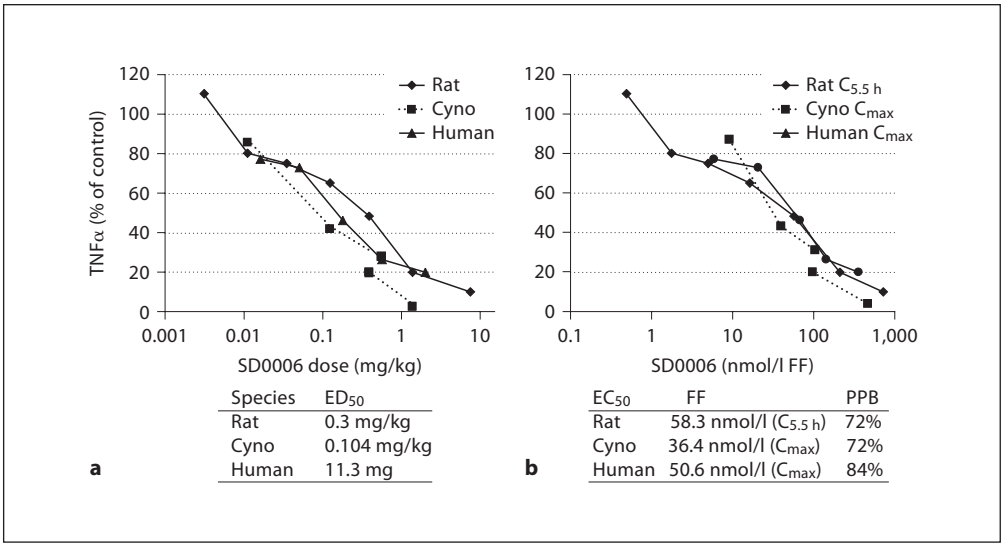

Fig. 12. Cross-species comparison for SD0006 inhibition of LPS-stimulated TNFα production. **a** Dose-response analysis. **b** Concentration-response analysis, with corrections for plasma protein binding (PPB) to give FF as shown. Human dosing was based on an assumption of approximately 70 kg per subject. Cyno = Cynomolgus monkey.

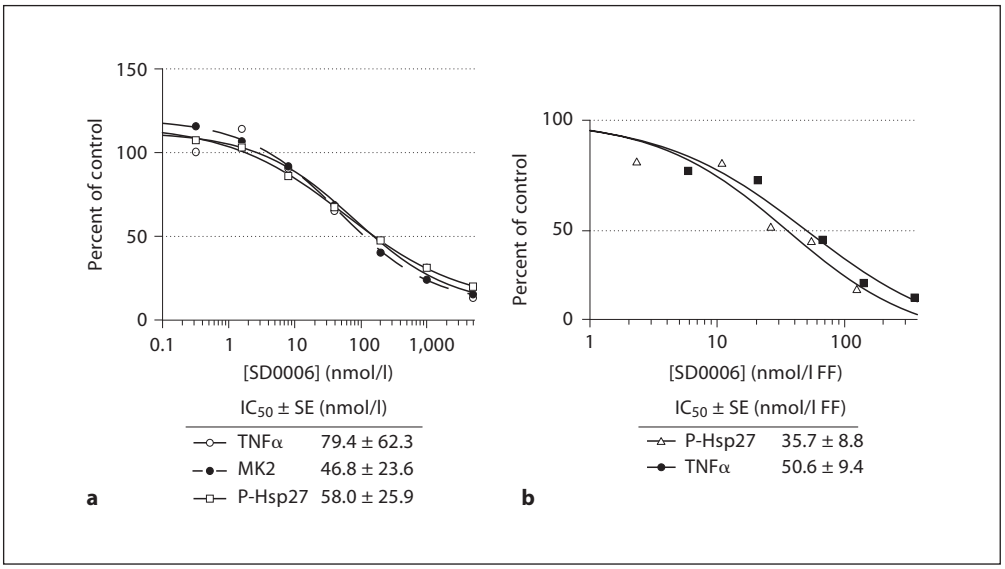

Fig. 13. SD0006 inhibition of p38α correlates to that of TNFα release ex vivo (**a**) and in vivo (**b**). Primary human monocytes were preincubated ex vivo with SD0006 for 60 min, challenged with LPS, then either medium was collected after 4 h to determine TNFα release as a mechanism biomarker, or cells were collected after 30 min, lysed and assayed for phosphorylation of MK-2 and Hsp27 as p38α target modulation biomarkers as described in Materials and Methods. p38α activities as determined by either MK-2 activity or P-Hsp27 assays, both have strong positive correlations with TNFα release, with their sample linear correlation coefficient ≥98% for both assays with TNFα. Each data point represents the average of 3 determinations, each from a different donor. For in vivo study, phase 1 clinical trial subjects were dosed 1 h prior to a 2 ng/kg LPS challenge as described in Materials and Methods. Blood collections near C_{max} were assayed for MK-2 activity as above. Curve fit, IC_{50} determinations, and standard errors (SE) were made using Grafit 5(2) software, with HWB values corrected for the FF in plasma. Each data point represents the average of 6 subjects.

Discussion

p38α is an attractive target for therapeutic intervention since it controls the expression of many inflammatory proteins. Based on encouraging results with the parent di-(4,5)-substituted diarylpyrazole (SC74102), a series of tri-(3,4,5)-substituted DAPs were synthesized and evaluated in vitro for better selectivity and potency as p38α inhibitors, and in vivo using rodent models of arthritis and the experimental endotoxemia model of LPS-induced acute inflammation in rodents, cynomolgus monkeys and humans. The most effective compound of this series, SD0006 (fig. 1), is described here. SD0006 had a moderate selectivity window against p38β and the best results in the rat SCW model (tables 1, 3), and was the first choice for in vivo studies, including evaluation in a phase 1 clinical trial.

The crystal structure of SC79659 (which gives the same binding conformation as SD0006) complexed with p38α showed that the inhibitor was bound at the ATP binding site (fig. 2), with the 4-chlorophenyl group bound tightly in a deeply buried lipophilic pocket that is apparently not utilized by ATP. This could confer to the greater kinase selectivity of SD0006 than of most ATP competitive inhibitors.

Others have reported that p38α inhibitors can inhibit the activation of p38α apparently by binding to the ATP pocket in the inactive state, which ATP cannot do, thus inducing a conformational change that blocks its activation by upstream MKKs [49]. Such inhibition of activation was observed with SD0006, at least in certain cell types, presumably by the aforementioned mechanism since SD0006 does not seem to inhibit MKK activities (table 1). p38α inhibitors have also been reported to enhance the activation of JNKs by inhibition of a feedback control where p38α phosphorylation of Tab1 inhibits the ability of TGF-β-activated kinase 1 to activate JNK [50]. SD0006 induced only minor activation of JNK at high concentrations. Activation of ERK has also been reported but was not observed here [51] (fig. 5).

We were able to demonstrate an excellent correlation between dose-dependent inhibition of p38α activity (by measuring either MK-2 activity or Hsp27 phosphorylation) and inhibition of TNFα release in human blood cells, both ex vivo and in vivo, in support of direct enzyme-to-cell translation (table 2, fig. 13). SD0006 IC_{50}s for enzyme inhibition in the biochemical in vitro kinase- and cell-based (U937, primary human monocytes, and HWB when corrected for the serum FF) TNFα release assays were comparable (tables 1, 2, fig. 3, 13). This indicated good cell permeability, a desirable trait for a potential clinical candidate. Good cross-species dose-response comparison between the rat and cynomolgus monkey enabled prediction of clinical dosing for humans (fig. 12). When corrected for plasma protein binding, the concentration-response curves for all 3 species overlapped.

RA joints are heavily infiltrated with monocytes and synoviocytes producing inflammatory protein. Induction of COX-2 expression by IL-1β in fibroblasts and by LPS in monocytes is known to be mediated by p38α [24, 55], and DAPs clearly suppressed both expression of COX-2 protein and of its inflammatory catalytic product, PGE_2 (fig. 4). Since these inhibitors do not affect COX-1 or COX-2 activity directly, the reduced PGE_2 release is solely a function of reduced COX-2 expression. Ex vivo and in vivo, SD0006 effectively inhibited the release of other inflammatory cytokines such as IL-1β and IL-6 (fig. 3, table 2). They also impressively inhibited many inflammatory and proteolytic proteins at the transcriptional level, and inhibition by SD0006 of rat SCW-induced arthritis closely mirrored that by the sTNFRII-Fc chimera (fig. 8). That the TNFα message was only modestly reduced by SD0006 was not surprising since most of the control of p38α over TNFα expression is known to be at the translational level [21]. All these results were in agreement with the roles of p38α in both TNFα and IL-1β production and signal transduction. Though the sTNFRII-Fc chimera also reduced the IL-6 and IL-1β message to the same level as SD0006, it has been reported that in some conditions anti-TNFα biologics may actually increase the levels of IL-6 [58]. Thus p38α inhibitors could possibly have broader anti-inflammatory efficacy than cytokine-targeted monotherapeutics like Humira or Anakinra.

SD0006 was effective in animal models of chronic inflammation and disease. In the carageenan rat paw model, SD0006 was shown to be effective in reducing both swelling and pain (fig. 6). In the murine CIA and rat SCW models of arthritis, DAPs were effective in reducing the incidence (fig. 7) and severity of disease (fig. 9, 10). Treatments were tolerated well with no obvious side effects, and were about equal to treatment with anti-rodent TNFα biologics (by anti-murine TNFα antibody in murine CIA, and by sTNFRII-Fc in rat SCW arthritis). This therapeutic parallelism between TNFα biologics and SD0006 underscores that the effectiveness of p38α inhibitors is mediated by suppression of inflammatory mediators such as TNFα. Most impressive were the radiographic results with SD0006, showing essentially normal joints and bone density in pretreated SCW rats. Bones of

the tibiotarsal joints were well defined with very little edema, resembling the normal controls (fig. 10a). It was also shown that bone mineral density in SCW rats was normalized using SD0006 (fig. 10b). Transcriptional suppression in SCW included proteins such as MMP13 and RANKL that are involved in the joint destruction resulting from RA (fig. 8). Bone density may also be protected by inhibition of cytokine signaling in osteoclast precursors. The bone-sparing mechanisms of SC79409 have been more extensively investigated and previously reported [57].

In summary, we have described SD0006, a DAP class p38α-selective inhibitor, and found a correlation between inhibition of p38α and inflammatory responses both ex vivo in human-cell-based assays and in vivo in human experimental endotoxemia. There was excellent agreement between preclinical studies and clinical results, with overlapping dose and concentration curves for rodents, monkeys, and humans. Oral efficacy was demonstrated in the CIA and SCW animal models of arthritis with clear radiographic evidence of joint and bone protection. Interaction of SD0006 with amino acids near but not in the ATP pocket that are unique to p38α gives it potency and selectivity advantages over most other ATP competitive inhibitors, and its ability to inhibit IL-1β and IL-6 in addition to TNFα potentially provides broader anti-inflammatory efficacy compared with cytokine-targeted monotherapeutics.

Acknowledgement

Pfizer Global Research and Development supported all research in this publication and employs all authors involved in the study.

References

1 Eigler A, Sinha B, Hartmann G, Endres S: Taming TNF: strategies to restrain this proinflammatory cytokine. Immunol Today 1997;18:487–492.
2 Barnes PJ: COPD: is there light at the end of the tunnel? Curr Opin Pharmacol 2004;4:263–272.
3 Shoelson SE, Herrero L, Naaz A: Obesity, inflammation, and insulin resistance. Gastroenterology 2007;132:2169–2180.
4 Taylor PC, Williams RO, Maini RN: Immunotherapy for rheumatoid arthritis. Curr Opin Immunol 2001;13:611–616.
5 Tobinick EL: Targeted etanercept for treatment-refractory pain due to bone metastasis: two case reports. Clin Ther 2003;25:2279–2288.
6 Sandborn WJ, Faubion WA: Biologics in inflammatory bowel disease: how much progress have we made? Gut 2004;53:1366–1373.
7 Vincek V, Jacob SE, Nassiri M, Herbert LM, Nadji M, Kerdel FA: Infliximab monotherapy in psoriasis: a case of rapid clinical and histological response. Int J Dermatol 2004;43:303–308.
8 Haraoui B: The anti-tumor necrosis factor agents are a major advance in the treatment of rheumatoid arthritis. J Rheumatol 2005;32:46–47.
9 Rott S, Mrowietz U: Recent developments in the use of biologics in psoriasis and autoimmune disorders. The role of autoantibodies. BMJ 2005;330:716–720.
10 Suryaprasad AG, Prindiville T: The biology of TNF blockade. Autoimmun Rev 2003;2:346–357.
11 Nurmohamed MT, Dijkmans BA: Efficacy, tolerability and cost effectiveness of disease-modifying antirheumatic drugs and biologic agents in rheumatoid arthritis. Drugs 2005;65:661–694.
12 Kroesen S, Widmer AF, Tyndall A, Hasler P: Serious bacterial infections in patients with rheumatoid arthritis under anti-TNF-α therapy. Rheumatology 2003;42:617–621.
13 Mohan AK, Cote TR, Siegel JN, Miles BM: Infectious complications of biologic treatments of rheumatoid arthritis. Curr Opin Rheumatol 2003;15:179–184.
14 Wolfe F, Michaud K: Lymphoma in rheumatoid arthritis: the effect of methotrexate and anti-tumor necrosis factor therapy in 18,572 patients. Arthritis Rheum 2004;50:1740–1751.
15 Ehlers S: Why does tumor necrosis factor targeted therapy reactivate tuberculosis? J Rheumatol 2005;32:35–39.
16 Hale KK, Trollinger D, Rihanek M, Manthey CL: Differential expression and activation of p38 mitogen-activated protein kinase α, β, γ, and δ in inflammatory cell lineages. J Immunol 1999;162:4246–4252.
17 Lee JC, Laydon JT, McDonnell PC, Gallagher TF, Kumar S, Green D, McNulty D, Blumenthal MJ, Heys JR, Landvatter SW, et al: A protein kinase involved in the regulation of inflammatory cytokine biosynthesis. Nature 1994;372:739–746.
18 Westra J, Doornbos-van der Meer B, de Boer P, van Leeuwen MA, van Rijswijk MH, Limburg PC: Strong inhibition of TNF-alpha production and inhibition of IL-8 and COX-2 mRNA expression in monocyte-derived macrophages by RWJ 67657, a p38 mitogen-activated protein kinase (MAPK) inhibitor. Arthritis Res Ther 2004;6:R384–R392.
19 Fijen JW, Zijlstra JG, De Boer P, Spanjersberg R, Tervaert JW, Van Der Werf TS, Ligtenberg JJ, Tulleken JE: Suppression of the clinical and cytokine response to endotoxin by RWJ-67657, a p38 mitogen-activated protein-kinase inhibitor, in healthy human volunteers. Clin Exp Immunol 2001;124:16–20.
20 Dean JL, Sully G, Clark AR, Saklatvala J: The involvement of AU-rich element-binding proteins in p38 mitogen-activated protein kinase pathway-mediated mRNA stabilisation. Cell Signal 2004;16:1113–1121.
21 Hitti E, Iakovleva T, Brook M, Deppenmeier S, Gruber AD, Radzioch D, Clark AR, Blackshear PJ, Kotlyarov A, Gaestel M: Mitogen-activated protein kinase-activated protein kinase 2 regulates tumor necrosis factor mRNA stability and translation mainly by altering tristetraprolin expression, stability, and binding to adenine/uridine-rich element. Mol Cell Biol 2006;26:2399–2407.
22 Manthey CL, Wang SW, Kinney SD, Yao Z: SB202190, a selective inhibitor of p38 mitogen-activated protein kinase, is a powerful regulator of LPS-induced mRNAs in monocytes. J Leukoc Biol 1998;64:409–417.
23 Miyazawa K, Mori A, Miyata H, Akahane M, Ajisawa Y, Okudaira H: Regulation of interleukin-1β-induced interleukin-6 gene expression in human fibroblast-like synoviocytes by p38 mitogen-activated protein kinase. J Biol Chem 1998;273:24832–24838.

24 Dean JL, Brook M, Clark AR, Saklatvala J: p38 mitogen-activated protein kinase regulates cyclooxygenase-2 mRNA stability and transcription in lipopolysaccharide-treated human monocytes. J Biol Chem 1999;274: 264–269.
25 Underwood DC, Osborn RR, Bochnowicz S, Webb EF, Rieman DJ, Lee JC, Romanic AM, Adams JL, Hay DWP, Griswold DE: SB 239063, a p38 MAPK inhibitor, reduces neutrophilia, inflammatory cytokines, MMP-9, and fibrosis in lung. Am J Physiol Lung Cell Mol Physiol 2000;279:L895–L902.
26 Clark AR, Dean JL, Saklatvala J: Post-transcriptional regulation of gene expression by mitogen-activated protein kinase p38. FEBS Lett 2003;546:37–44.
27 Huang H, Rose JL, Hoyt DG: p38 mitogen-activated protein kinase mediates synergistic induction of inducible nitric-oxide synthase by lipopolysaccharide and interferon-γ through signal transducer and activator of transcription 1 ser727 phosphorylation in murine aortic endothelial cells. Mol Pharmacol 2004;66:302–311.
28 Westra J, Limburg P, deBoer P, vanRijswijk M: Effects of RWJ 67657, a p38 mitogen activated protein kinase (MAPK) inhibitor, on the production of inflammatory mediators by rheumatoid synovial fibroblasts. Ann Rheum Dis 2004;63:1453–1459.
29 Takami M, Cho ES, Lee SY, Kamijo R, Yim M: Phosphodiesterase inhibitors stimulate osteoclast formation via TRANCE/RANKL expression in osteoblasts: possible involvement of ERK and p38 MAPK pathways. FEBS Lett 2005;579:832–838.
30 Vanden Berghe W, Vermeulen L, De Wilde G, De Bosscher K, Boone E, Haegeman G: Signal transduction by tumor necrosis factor and gene regulation of the inflammatory cytokine interleukin-6. Biochem Pharmacol 2000;60:1185–1195.
31 Badger AM, Griswold DE, Kapadia R, Blake S, Swift BA, Hoffman SJ, Stroup GB, Webb E, Rieman DJ, Gowen M, Boehm JC, Adams JL, Lee JC: Disease-modifying activity of SB 242235, a selective inhibitor of p38 mitogen-activated protein kinase, in rat adjuvant-induced arthritis. Arthritis Rheum 2000;43: 175–183.
32 McLay IM, Halley F, Souness JE, McKenna J, Benning V, Birrell M, Burton B, Belvisi M, Collis A, Constan A: The discovery of RPR 200765A, a p38 MAP kinase inhibitor displaying a good oral anti-arthritic efficacy. Bioorg Med Chem 2001;9:537–554.
33 Branger J, van den Blink B, Weijer S, Madwed J, Bos CL, Gupta A, Yong CL, Polmar SH, Olszyna DP, Hack CE, van Deventer SJH, Peppelenbosch MP, van der Poll T: Anti-inflammatory effects of a p38 mitogen-activated protein kinase inhibitor during human endotoxemia. J Immunol 2002;168: 4070–4077.
34 Regan J, Breitfelder S, Cirillo P, Gilmore T, Graham AG, Hickey E, Klaus B, Madwed J, Moriak M, Moss N, Pargellis C, Pav S, Proto A, Swinamer A, Tong L, Torcellini C: Pyrazole urea-based inhibitors of p38 MAP kinase: from lead compound to clinical candidate. J Med Chem 2002;45:2994–3008.
35 Revesz L, Blum E, Di Padova FE, Buhl T, Feifel R, Gram H, Hiestand P, Manning U, Rucklin G: Novel p38 inhibitors with potent oral efficacy in several models of rheumatoid arthritis. Bioorg Med Chem Lett 2004;14: 3595–3599.
36 Stelmach JE, Liu L, Patel SB, Pivnichny JV, Scapin G, Singh S, Hop CECA, Wang Z, Strauss JR, Cameron PM: Design and synthesis of potent, orally bioavailable dihydroquinazolinone inhibitors of p38 MAP kinase. Bioorg Med Chem Lett 2003;13: 277–280.
37 Kumar S, Boehm J, Lee JC: p38 MAP kinases: key signalling molecules as therapeutic targets for inflammatory diseases. Nat Rev Drug Discov 2003;2:717–726.
38 Saklatvala J: The p38 MAP kinase pathway as a therapeutic target in inflammatory disease. Curr Opin Pharmacol 2004;4:372–377.
39 Liverton NJ, Butcher JW, Claiborne CF, Claremon DA, Libby BE, Nguyen KT, Pitzenberger SM, Selnick HG, Smith GR, Tebben A, Vacca JP, Varga SL, Agarwal L, Dancheck K, Forsyth AJ, Fletcher DS, Frantz B, Hanlon WA, Harper CF, Hofsess SJ, Kostura M, Lin J, Luell S, O'Neill EA, O'Keefe SJ, et al: Design and synthesis of potent, selective, and orally bioavailable tetrasubstituted imidazole inhibitors of p38 mitogen-activated protein kinase. J Med Chem 1999;42:2180–2190.
40 Jackson PF, Bullington JL: Pyridinylimidazole based p38 MAP kinase inhibitors. Curr Top Med Chem 2002;2:1011–1020.
41 de Laszlo SE, Visco D, Agarwal L, Chang L, Chin J, Croft G, Forsyth A, Fletcher D, Frantz B, Hacker C: Pyrroles and other heterocycles as inhibitors of p38 kinase. Bioorg Med Chem Lett 1998;8:2689–2694.
42 Henry JR, Rupert KC, Dodd JH, Turchi IJ, Wadsworth SA, Cavender DE, Schafer PH, Siekierka JJ: Potent inhibitors of the MAP kinase p38. Bioorg Med Chem Lett 1998;8: 3335–3340.
43 Haddad JJ: VX-745. Vertex Pharmaceuticals. Curr Opin Investig Drugs 2001;2:1070–1076.
44 Otwinowski Z, Minor M: Processing of X-ray diffraction data collected in oscillation mode. Methods Enzymol 1997;276A:307–326.
45 Zhang F, Strand A, Robbins D, Cobb MH, Goldsmith EJ: Atomic structure of the MAP kinase ERK2 at 2.3 Å resolution. Nature 1994;367:704–711.
46 Jones TA, Zou JY, Cowan SW, Kjeldgaard M: Improved methods for building protein models in electron density maps and the location of errors in these models. Acta Crystallogr A 1991;47(pt 2):110–119.
47 Brunger AT: X-PLOR (Version 3.1): A System for X-Ray Crystallography and NMR. New Haven, Yale University Press, 1993.
48 Hemmer W, McGlone M, Tsigelny I, Taylor SS: Role of the glycine triad in the ATP-binding site of cAMP-dependent protein kinase. J Biol Chem 1997;272:16946–16954.
49 Frantz B, Klatt T, Pang M, Parsons J, Rolando A, Williams H, Tocci MJ, O'Keefe SJ, O'Neill EA: The activation state of p38 mitogen-activated protein kinase determines the efficiency of ATP competition for pyridinylimidazole inhibitor binding. Biochemistry 1998;37:13846–13853.
50 Cheung PCF, Campbell DG, Nebreda AR, Cohen P: Feedback control of the protein kinase TAK1 by SAPK2a/p38α. EMBO J 2003; 22:5793–5805.
51 Henklova P, Vrzal R, Papouskova B, Bednar P, Jancova P, Anzenbacherova E, Ulrichova J, Maurel P, Pavek P, Dvorak Z: SB203580, a pharmacological inhibitor of p38 MAP kinase transduction pathway activates ERK and JNK MAP kinases in primary cultures of human hepatocytes. Eur J Pharmacol 2008;593:16–23.
52 Telliez A, Furman C, Pommery N, Henichart JP: Mechanisms leading to COX-2 expression and COX-2 induced tumorigenesis: topical therapeutic strategies targeting COX-2 expression and activity. Anticancer Agents Med Chem 2006;6:187–208.
53 Williams R: Collagen-induced arthritis in mice. Methods Mol Med 2007;136:191–199.
54 Schwab J, Anderle S, Brown R, Dalldorf F, Thompson R: Pro- and anti-inflammatory roles of interleukin-1 in recurrence of bacterial cell wall-induced arthritis in rats. Infect Immun 1991;59:4436–4442.
55 Jacques C, Gosset M, Berenbaum F, Gabay C, Gerald L: The role of IL-1 and IL-1Ra in joint inflammation and cartilage degradation. Vitam Horm 2006;74:371–403.
56 Lam J, Takeshita S, Barker JE, Kanagawa O, Ross P, Teitelbaum SL: TNF-α induces osteoclastogenesis by direct stimulation of macrophages exposed to permissive levels of RANK ligand. J Clin Invest 2000;106:1481–1488.
57 Mbalaviele G, Anderson G, Jones A, De Ciechi P, Settle S, Mnich S, Thiede M, Abu-Amer Y, Portanova J, Monahan J: Inhibition of p38 mitogen-activated protein kinase prevents inflammatory bone destruction. J Pharmacol Exp Ther 2006;317:1044–1053.
58 Haugen E, Scharin Täng M, Isic A, Andersson B, Fu M: TNFα antagonist upregulates interleukin-6 in rats with hypertensive heart failure. Int J Cardiol 2008;130:64–68.